3D automatic methods to segment “virtual” endocasts: state of the art and future directions

Gérard SUBSOL[1]
Gilles GESQUIERE[2]
José BRAGA[3]
Francis THACKERAY[4]

.

1 *Lab. of Computer Science LIRMM, CNRS / University Montpellier 2, France*
HOPE Team France / South Africa

2 *Lab. of Computer Science LSIS, Aix-Marseille University - IUT Provence, Arles, France*

3 *Lab. of Anthropobiology AMIS, University Paul Sabatier, Toulouse, France*
HOPE Team France / South Africa

4 *Institute for Human Evolution, University of the Witwatersrand, South Africa*
HOPE Team France / South Africa

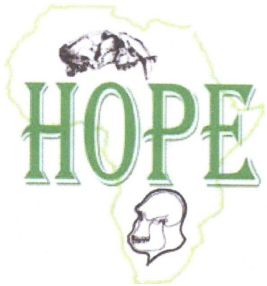

Manual methods

Endocranial Features of *Australopithecus africanus* Revealed by 2- and 3-D Computed Tomography

GLENN C. CONROY,* MICHAEL W. VANNIER, PHILLIP V. TOBIAS

The earliest hominid from South Africa, *Australopithecus africanus*, is known from only six specimens in which accurate assessment of endocranial capacity and cranial venous outflow pattern can be obtained. This places a severe limit on a number of hypotheses concerning early hominid evolution, particularly those involving brain–body size relationships and adaptations of the circulatory system to evolving upright posture. Advances in high-resolution two- and three-dimensional computed tomography (CT) now allow the inclusion of another important specimen to this list, MLD 37/38 from Makapansgat. A new computer imaging technique is described that "reconstructs" the missing portions of the endocranial cavity in order to determine endocranial capacity. In addition, CT evaluation allows assessment of cranial venous outflow pattern even in cases where the endocranial cavity is completely filled with stone matrix. Results show that endocranial capacity in this specimen is less than originally proposed and also support the view that gracile and robust australopithecines evolved different cranial venous outflow patterns in response to upright postures.

Science, Vol. 247, February 1990

- CT-Scan of MLD37/38: slice thickness = 2 mm
- **Draw manually** the endocranial Region Of Interest **slice by slice** with a graphics pad
- Draw the missing frontal cortex by symmetry and assessing it with 3D reconstructions

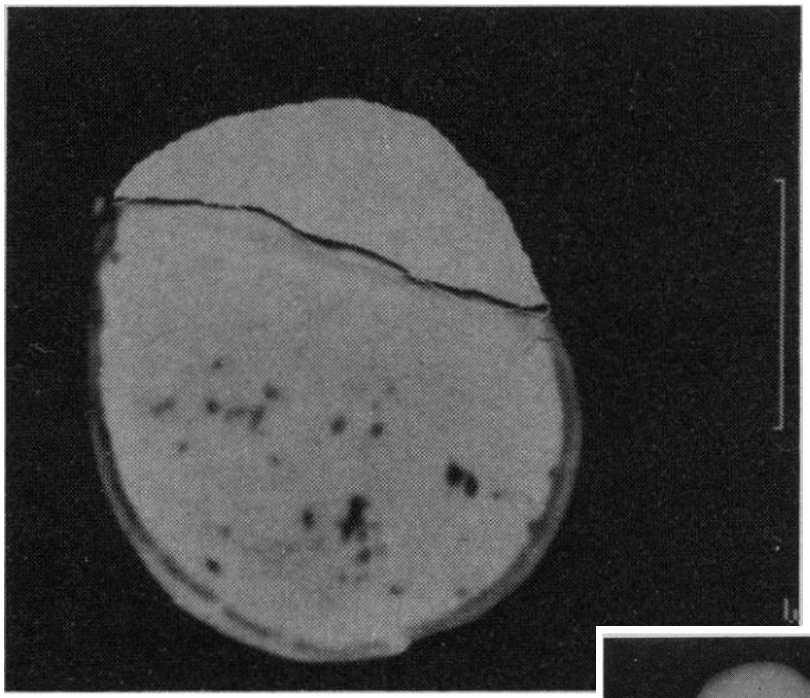

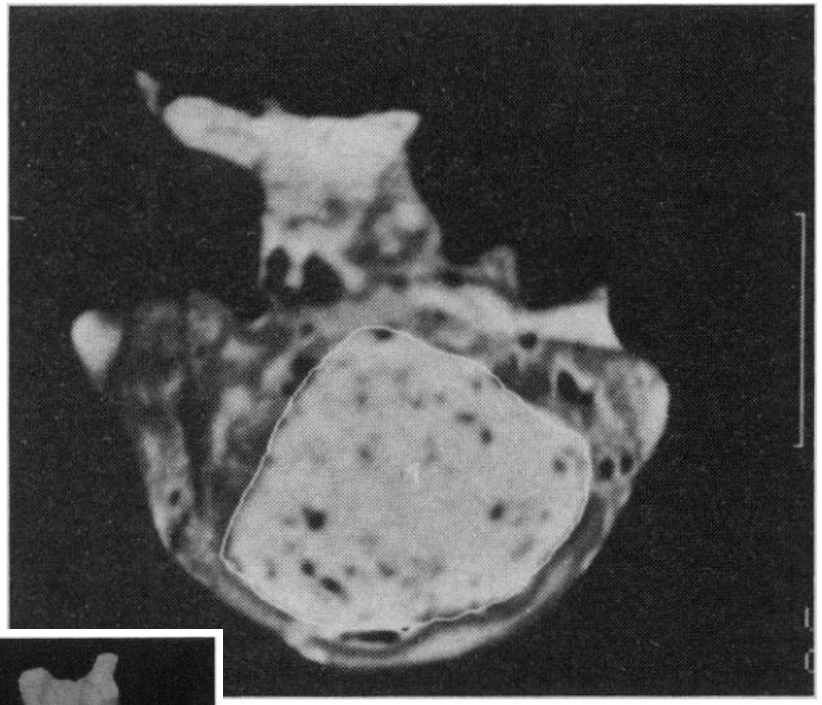

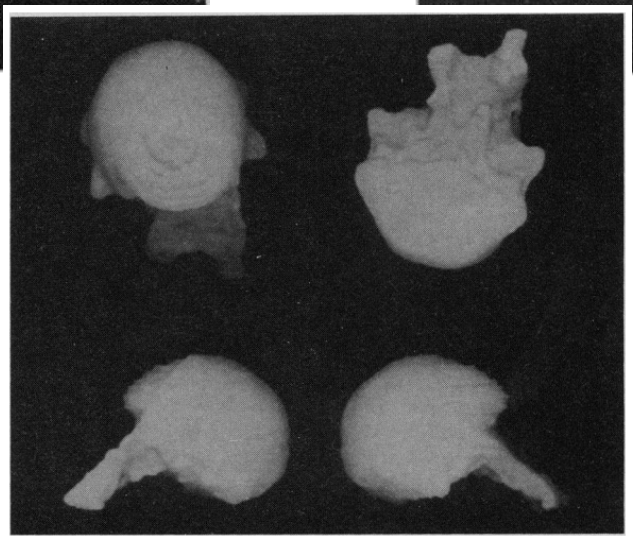

Computer-assisted methods (1)

Endocranial Capacity in an Early Hominid Cranium from Sterkfontein, South Africa

Glenn C. Conroy,* Gerhard W. Weber, Horst Seidler,
Phillip V. Tobias, Alex Kane, Barry Brunsden

Two- and three-dimensional computer imaging shows that endocranial capacity in an ~2.8- to 2.6-million-year-old early hominid cranium (Stw 505) from Sterkfontein, South Africa, tentatively assigned to *Australopithecus africanus*, is ~515 cubic centimeters. Although this is the largest endocranial capacity recorded for this species, it is still markedly less than anecdotal reports of endocranial capacity exceeding 600 cubic centimeters. No australopithecine has an endocranial capacity approaching, let alone exceeding, 600 cubic centimeters. Some currently accepted estimates of early hominid endocranial capacity may be inflated, suggesting that the tempo and mode of early hominid brain evolution may need reevaluation.

Science, Vol. 280, June 1998

- CT-Scan of Stw 505: voxel size 0.39 x 0.39 x 1 mm
- **Use a 3D image processing software** (Analyze)

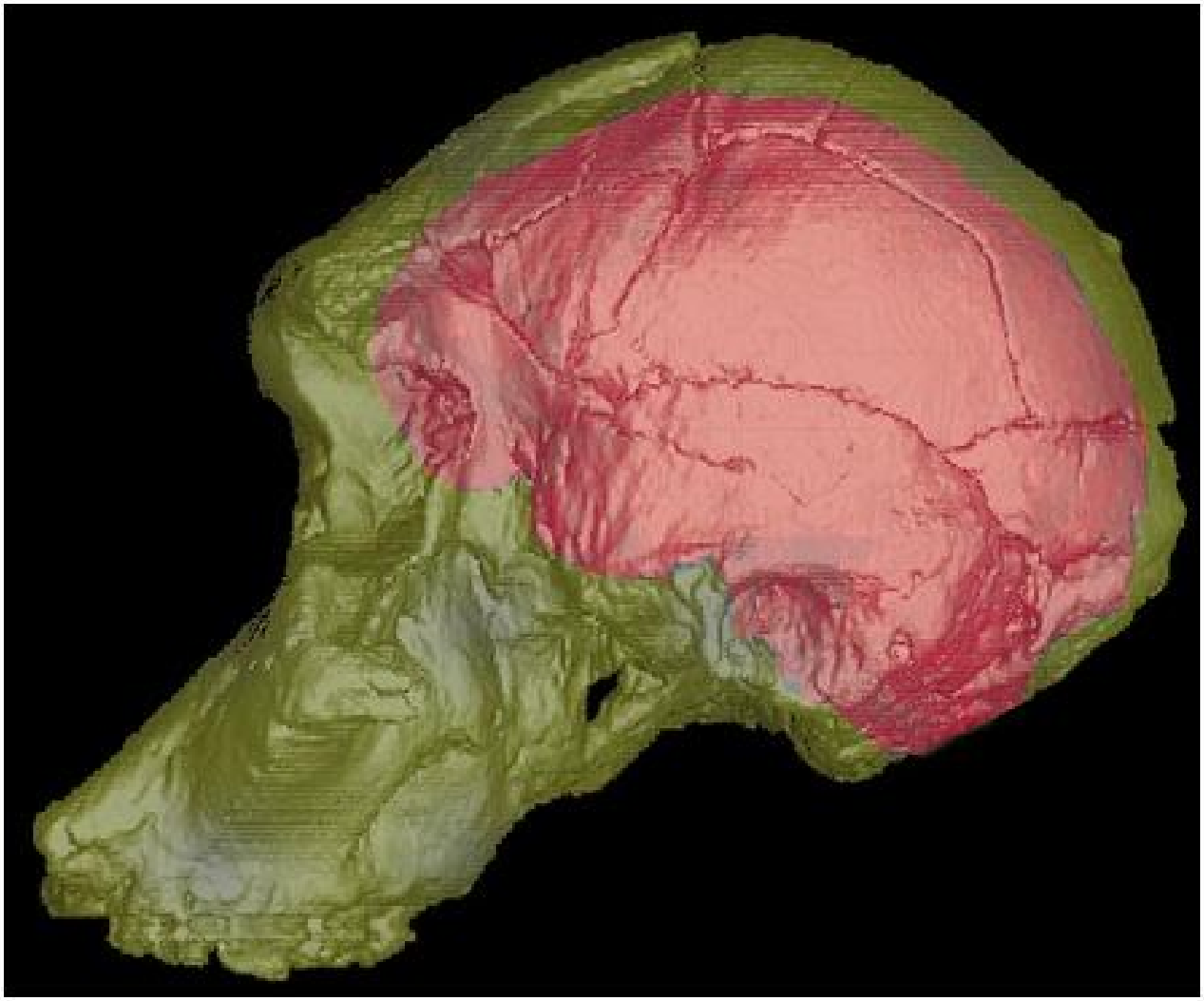

Computer-assisted methods (2)

WILEY InterScience®

AMERICAN JOURNAL OF PHYSICAL ANTHROPOLOGY 132:183–192 (2007)

Validation of Plaster Endocast Morphology Through 3D CT Image Analysis

P. Thomas Schoenemann,[1,2*] James Gee,[3] Brian Avants,[3] Ralph L. Holloway,[4] Janet Monge,[2,5] and Jason Lewis[6]

[1]*Department of Behavioral Sciences, University of Michigan-Dearborn, Dearborn, MI 48128*
[2]*Museum of Archaeology and Anthropology, University of Pennsylvania, Philadelphia, PA 19104*
[3]*Department of Radiology, University of Pennsylvania, Philadelphia, PA 19104*
[4]*Department of Anthropology, Columbia University, New York, NY 10027*
[5]*Department of Anthropology, University of Pennsylvania, Philadelphia, PA 19104*
[6]*Department of Anthropological Sciences, Stanford University, Stanford, CA 94305*

KEY WORDS CT; computed tomography; endocast; validation

ABSTRACT A crucial component of research on brain evolution has been the comparison of fossil endocranial surfaces with modern human and primate endocrania. The latter have generally been obtained by creating endocasts out of rubber latex shells filled with plaster. The extent to which the method of production introduces errors in endocast replicas is unknown. We demonstrate a powerful method of comparing complex shapes in 3-dimensions (3D) that is broadly applicable to a wide range of paleoanthropological questions. Pairs of virtual endocasts (VEs) created from high-resolution CT scans of corresponding latex/plaster endocasts and their associated crania were rigidly registered (aligned) in 3D space for two *Homo sapiens* and two *Pan troglodytes* specimens. Distances between each cranial VE and its corresponding latex/plaster VE were then mapped on a voxel-by-voxel basis. The results show that between 79.7% and 91.0% of the voxels in the four latex/plaster VEs are within 2 mm of their corresponding cranial VEs surfaces. The average error is relatively small, and variation in the pattern of error across the surfaces appears to be generally random overall. However, inferior areas around the cranial base and the temporal poles were somewhat overestimated in both human and chimpanzee specimens, and the area overlaying Broca's area in humans was somewhat underestimated. This study gives an idea of the size of possible error inherent in latex/plaster endocasts, indicating the level of confidence we can have with studies relying on comparisons between them and, e.g., hominid fossil endocasts. Am J Phys Anthropol 132:183–192, 2007.

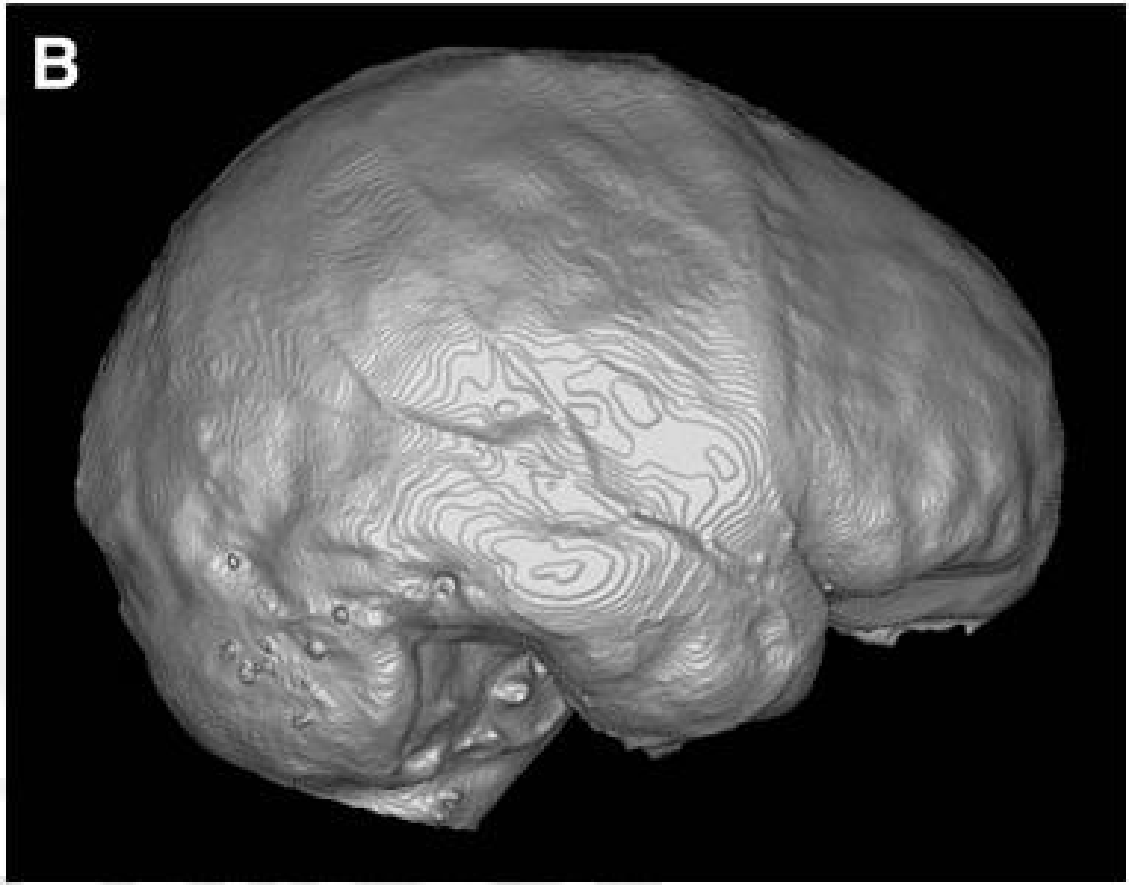

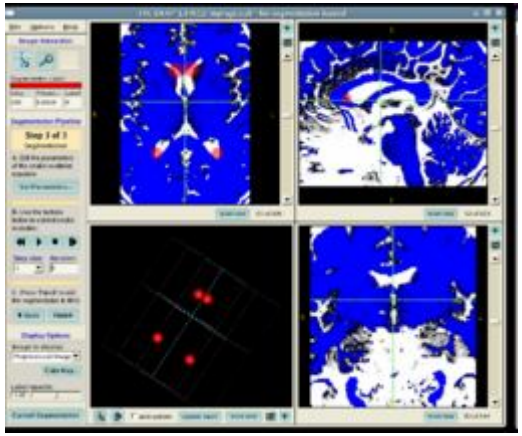

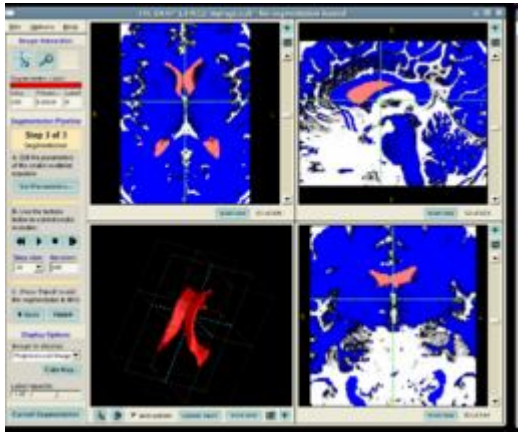

- Voxel size ~ 0.4 mm × 0.4 mm × 1.0 mm
- Use **the free software** ITK-Snap (3D-level set) *http://www.itksnap.org*
  - Requires a lot of manual interaction to place seed balloons and tune parameters
  - Requires to manually "cut" the surface which went through holes (in particular at the level of the foramen) → introduce errors and user-dependency
  - May fail to process very large images

Requirements for endocast segmentation

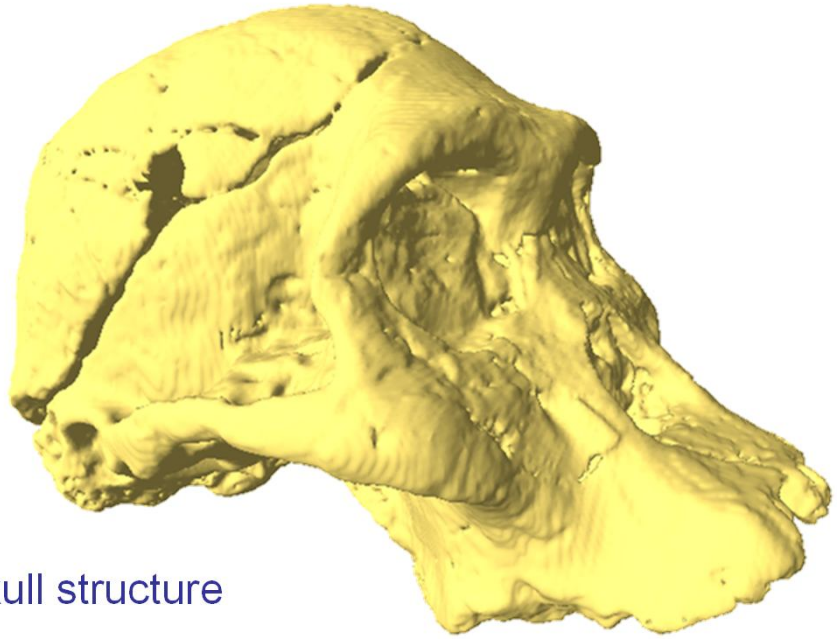

1. **Differentiating matrix and bone**
   - Very specific to the fossil.
   - General problem which concerns all the skull structure
   - No general solution

2. Dealing with the **holes** (anatomical holes as well as cracks or small missing parts)
   - To minimize the user interaction

3. Dealing with **large images** (e.g. acquired by µ-CT)
   - To process future images

An automated method

- Based on the **deformable (or active) surface paradigm** introduced in image processing.
- Used in particular to segment the brain surface in MRI images (*Freesurfer*).
- Already demonstrated to segment virtual endocast in *J. Montagnat "Modèles déformables pour la segmentation et la modélisation d'images médicales 3D et 4D" PhD Thesis Nice-Sophia Antipolis University, France (1999)*.

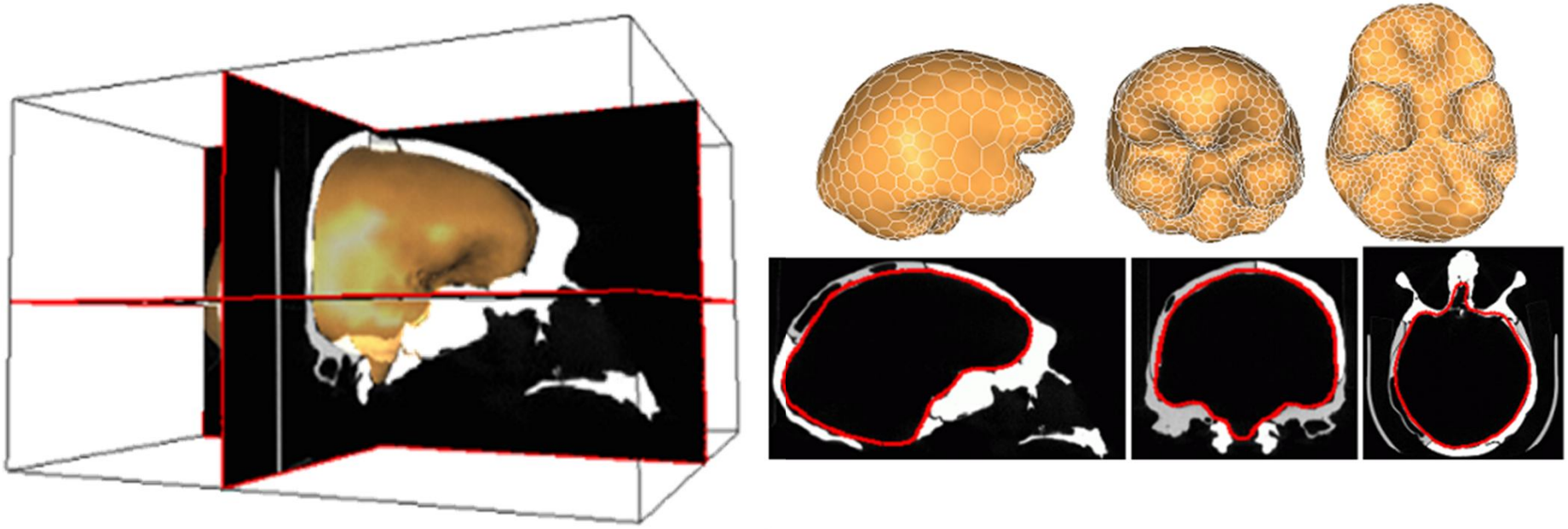

Principle of the method

- The data are represented by a set of 3D points

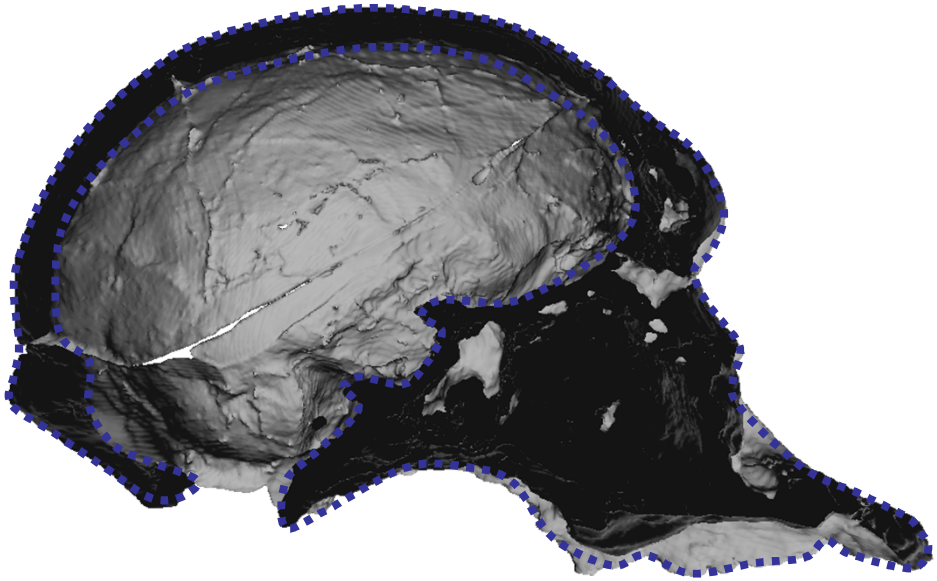

Principle of the method

- The data are represented by a set of 3D points

- Let a simple closed surface mesh composed of 3D vertices $\boldsymbol{P_i}$ (e.g. a sphere)

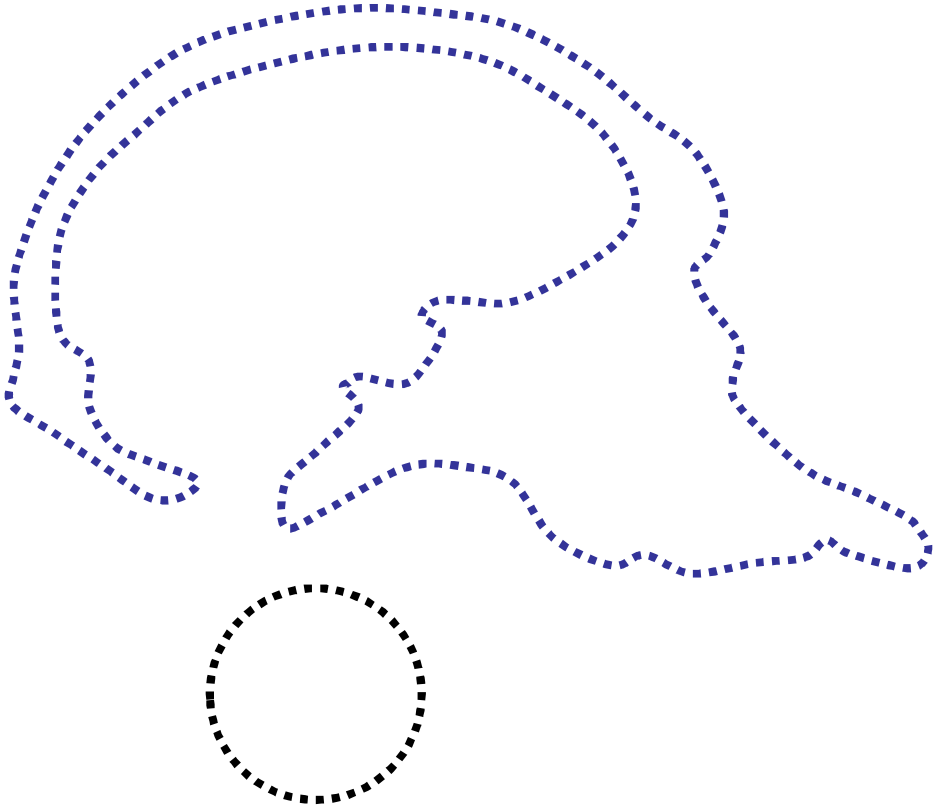

Principle of the method

- The data are represented by a set of 3D points
- Let a simple closed surface mesh composed of 3D vertices $\boldsymbol{P_i}$ (e.g. a sphere)
- The surface mesh is initially positioned "in the middle" of the data

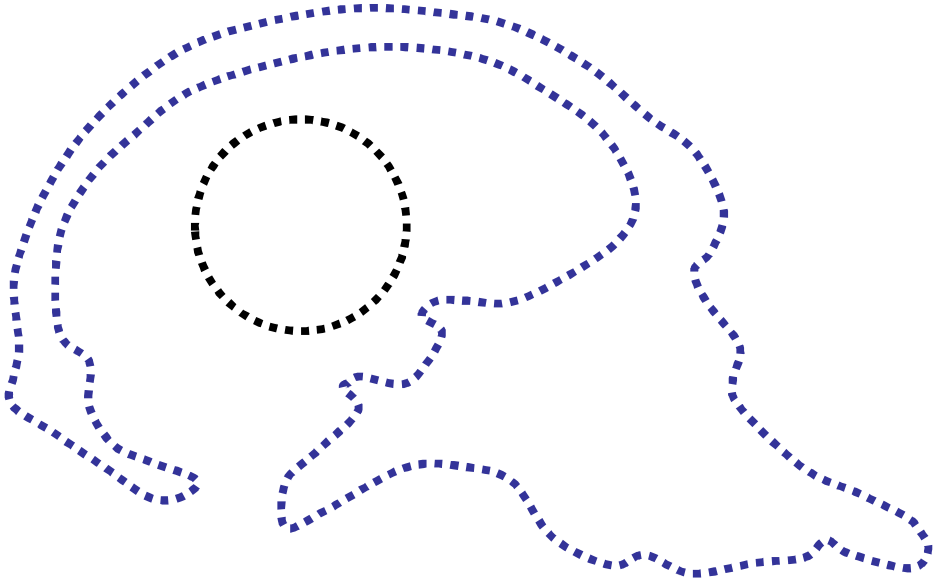

Principle of the method

- The data are represented by a set of 3D points
- Let a simple closed surface mesh composed of 3D vertices $\boldsymbol{P_i}$ (e.g. a sphere)
- The surface mesh is initially positioned "in the middle" of the data
- This surface will deform under the influence of:
  - an external force $\mathbf{F}_{ext}$ which attracts the vertices $\boldsymbol{P_i}$ towards the data
  - an internal force $\mathbf{F}_{int}$ which tends to keep the surface smooth (e.g. curvature continuity)

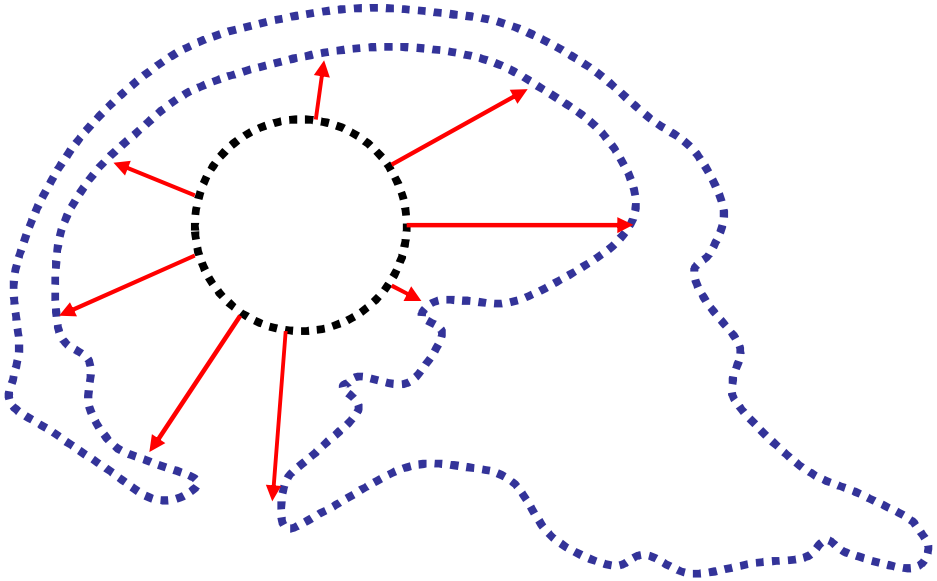

Principle of the method

- The data are represented by a set of 3D points
- Let a simple closed surface mesh composed of 3D vertices P_i (e.g. a sphere)
- The surface mesh is initially positioned "in the middle" of the data
- This surface will deform under the influence of:
  - an external force $\mathbf{F}_{ext}$ which attracts the vertices P_i towards the data
  - an internal force $\mathbf{F}_{int}$ which tends to keep the surface smooth (e.g. curvature continuity)

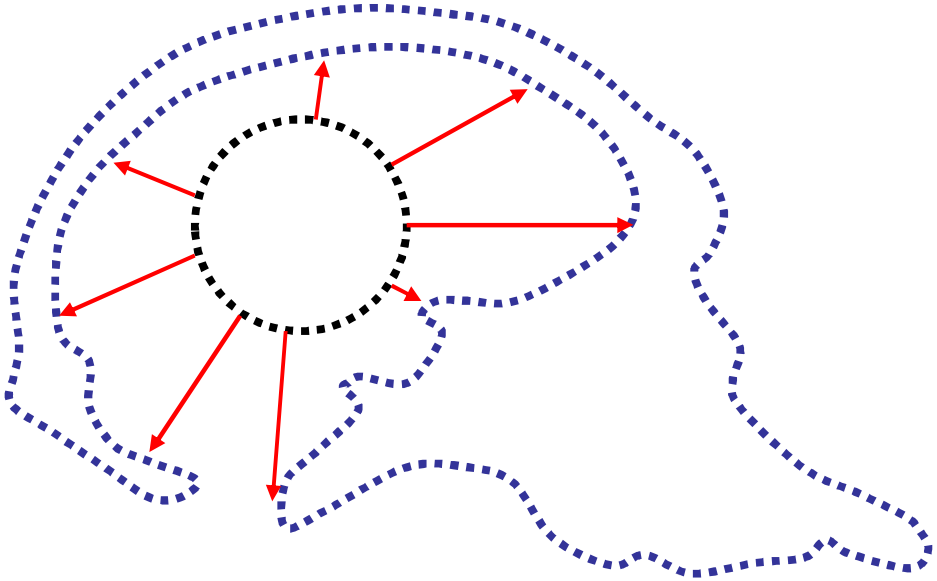

- At time t, all the vertices P_i follow the evolution law:

$$P_i^{t+1} = P_i^t + (1-\gamma)(P_i^t - P_i^{t-1}) + \alpha_i \mathbf{F}_{int} + \beta_i \mathbf{F}_{ext}$$

Principle of the method

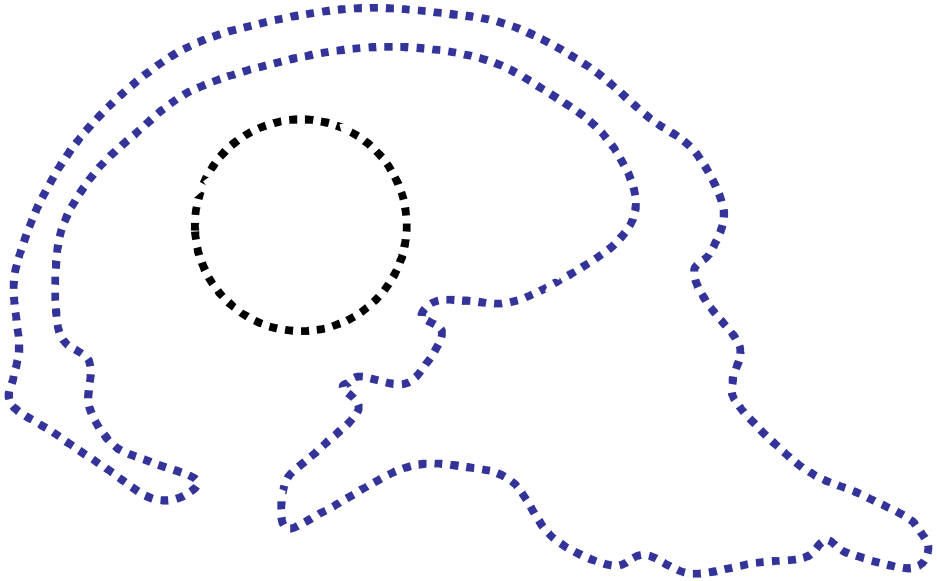

- The data are represented by a set of 3D points
- Let a simple closed surface mesh composed of 3D vertices P_i (e.g. a sphere)
- The surface mesh is initially positioned "in the middle" of the data
- This surface will deform under the influence of:
  - an external force $\mathbf{F}_{ext}$ which attracts the vertices P_i towards the data
  - an internal force $\mathbf{F}_{int}$ which tends to keep the surface smooth (e.g. curvature continuity)

- At time t, all the vertices P_i follow the evolution law:

$$P_i^{t+1} = P_i^t + (1-\gamma)(P_i^t - P_i^{t-1}) + \alpha_i \mathbf{F}_{int} + \beta_i \mathbf{F}_{ext}$$

- Iterate the process until the vertices P_i do not move anymore.

Principle of the method

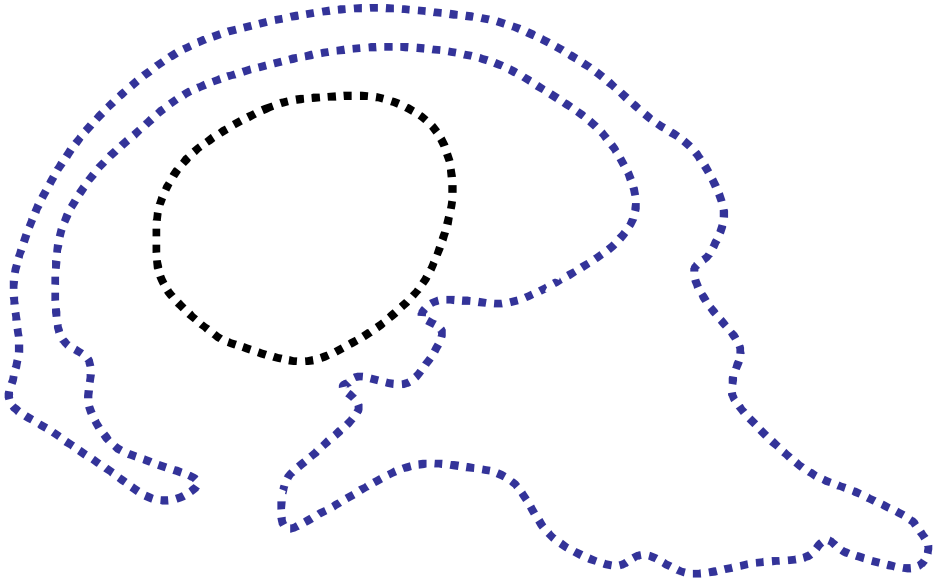

- The data are represented by a set of 3D points
- Let a simple closed surface mesh composed of 3D vertices P_i (e.g. a sphere)
- The surface mesh is initially positioned "in the middle" of the data
- This surface will deform under the influence of:
  - an external force $\mathbf{F}_{ext}$ which attracts the vertices P_i towards the data
  - an internal force $\mathbf{F}_{int}$ which tends to keep the surface smooth (e.g. curvature continuity)

- At time t, all the vertices P_i follow the evolution law:

$$P_i^{t+1} = P_i^t + (1-\gamma)(P_i^t - P_i^{t-1}) + \alpha_i \mathbf{F}_{int} + \beta_i \mathbf{F}_{ext}$$

- Iterate the process until the vertices P_i do not move anymore.

Principle of the method

- The data are represented by a set of 3D points

- Let a simple closed surface mesh composed of 3D vertices P_i (e.g. a sphere)

- The surface mesh is initially positioned "in the middle" of the data

- This surface will deform under the influence of:

  - an external force $\mathbf{F}_{ext}$ which attracts the vertices P_i towards the data
  - an internal force $\mathbf{F}_{int}$ which tends to keep the surface smooth (e.g. curvature continuity)

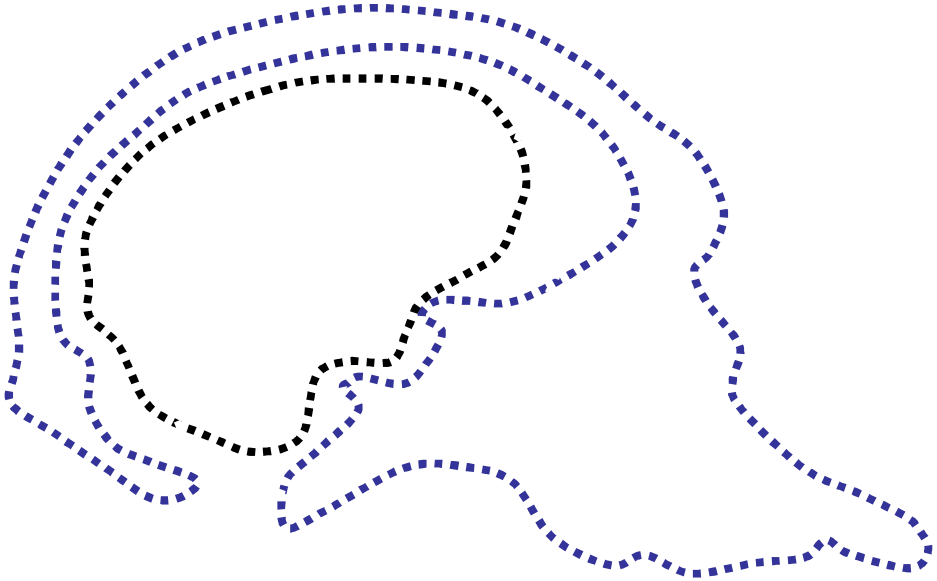

- At time t, all the vertices P_i follow the evolution law:

$$P_i^{t+1} = P_i^t + (1-\gamma)(P_i^t - P_i^{t-1}) + \alpha_i \mathbf{F}_{int} + \beta_i \mathbf{F}_{ext}$$

- Iterate the process until the vertices P_i do not move anymore.

Principle of the method

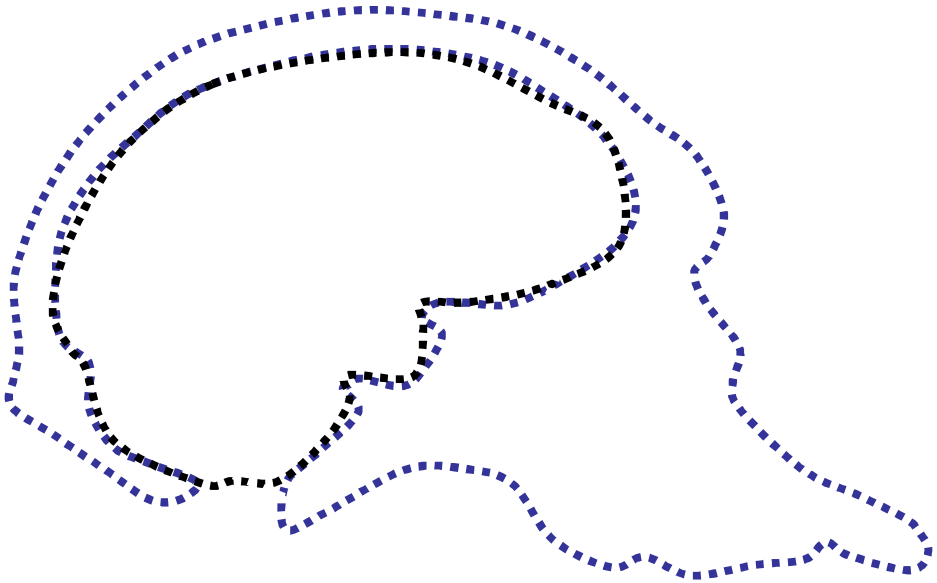

- The data are represented by a set of 3D points
- Let a simple closed surface mesh composed of 3D vertices P_i (e.g. a sphere)
- The surface mesh is initially positioned "in the middle" of the data
- This surface will deform under the influence of:
  - an external force $\mathbf{F}_{ext}$ which attracts the vertices P_i towards the data
  - an internal force $\mathbf{F}_{int}$ which tends to keep the surface smooth (e.g. curvature continuity)

- At time t, all the vertices P_i follow the evolution law:

$$P_i^{t+1} = P_i^t + (1-\gamma)(P_i^t - P_i^{t-1}) + \alpha_i \mathbf{F}_{int} + \beta_i \mathbf{F}_{ext}$$

- Iterate the process until the vertices P_i do not move anymore.

Principle of the method

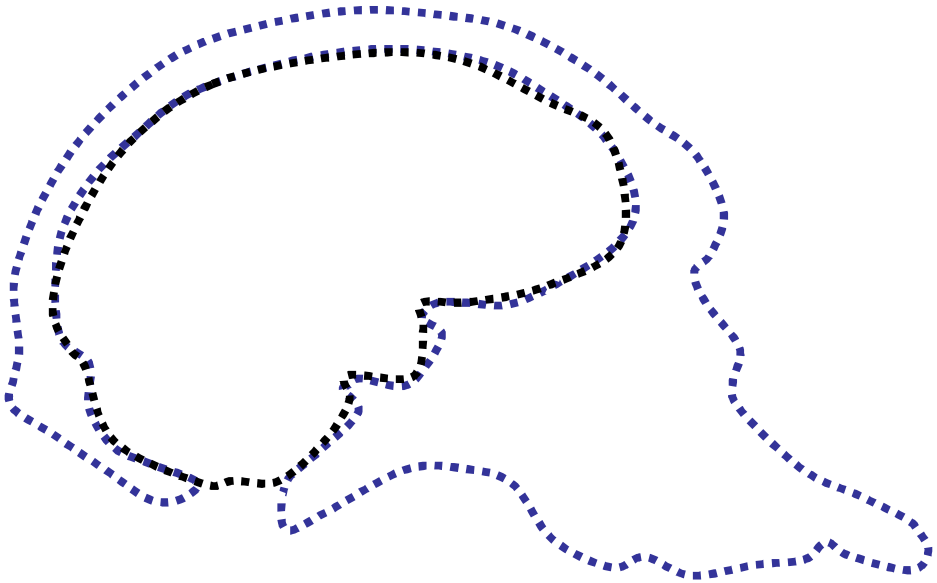

- The data are represented by a set of 3D points
- Let a simple closed surface mesh composed of 3D vertices P_i (e.g. a sphere)
- The surface mesh is initially positioned "in the middle" of the data
- This surface will deform under the influence of:
  - an external force $\mathbf{F}_{ext}$ which attracts the vertices P_i towards the data
  - an internal force $\mathbf{F}_{int}$ which tends to keep the surface smooth (e.g. curvature continuity)

- At time t, all the vertices P_i follow the evolution law:

$$P_i^{t+1} = P_i^t + (1-\gamma)(P_i^t - P_i^{t-1}) + \alpha_i \mathbf{F}_{int} + \beta_i \mathbf{F}_{ext}$$

- Iterate the process until the vertices P_i do not move anymore.
- Eventually, add more vertices in the mesh when the distance between the existing vertices becomes too large in order to recover the details.

Principle of the method

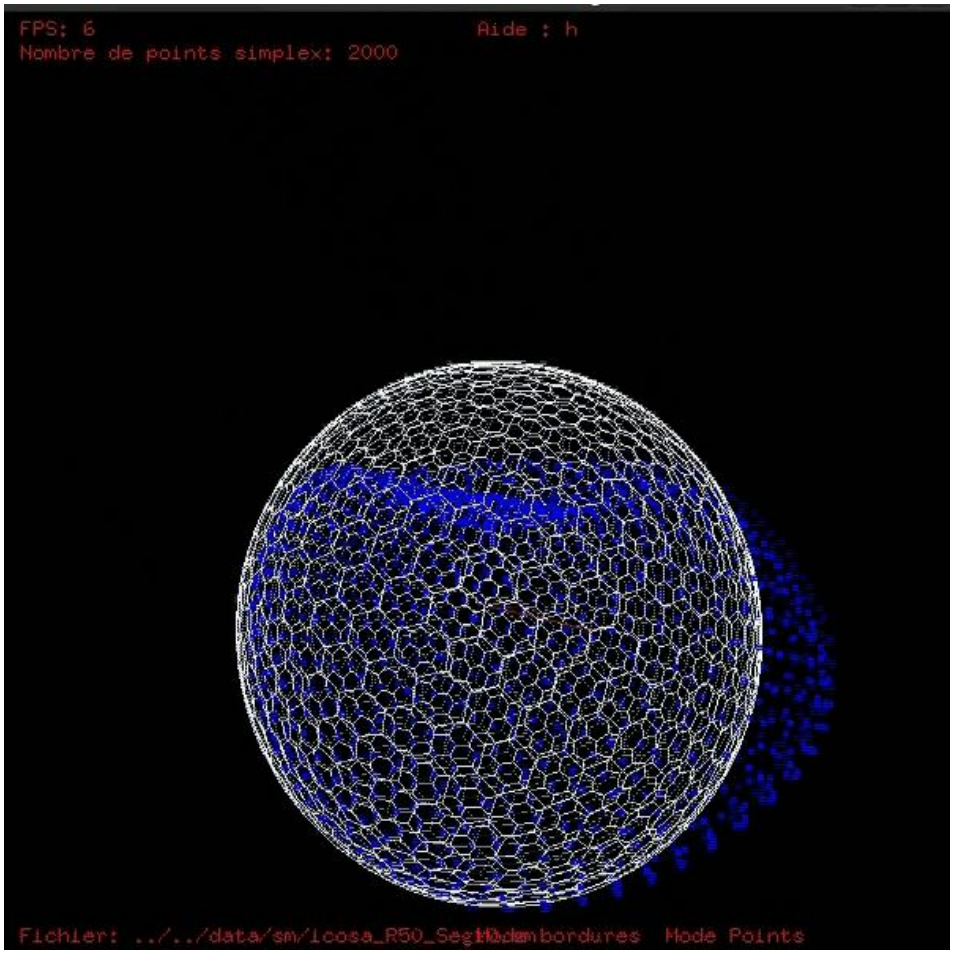

- The data are represented by a set of 3D points
- Let a simple closed surface mesh composed of 3D vertices $\boldsymbol{P_i}$ (e.g. a sphere)
- The surface mesh is initially positioned "in the middle" of the data
- This surface will deform under the influence of:
  - an external force $\mathbf{F}_{ext}$ which attracts the vertices $\boldsymbol{P_i}$ towards the data
  - an internal force $\mathbf{F}_{int}$ which tends to keep the surface smooth (e.g. curvature continuity)
- At time t, all the vertices $\boldsymbol{P_i}$ follow the evolution law:

$$P_i^{t+1} = P_i^t + (1-\gamma)(P_i^t - P_i^{t-1}) + \alpha_i \mathbf{F}_{int} + \beta_i \mathbf{F}_{ext}$$

- Iterate the process until the vertices $\boldsymbol{P_i}$ do not move anymore.
- Eventually, add more vertices in the mesh when the distance between the existing vertices becomes too large in order to recover the details.

Pan paniscus

- *A. Balzeau, E. Gilissen et al. "Internal cranial anatomy of the type specimen of Pan paniscusand available data for study". Journal of Human Evolution 56, 205–208 (2009)*
- Data: 857,720 points
- Downloaded from *http://www.metafro.be/primates/panpaniscustype*

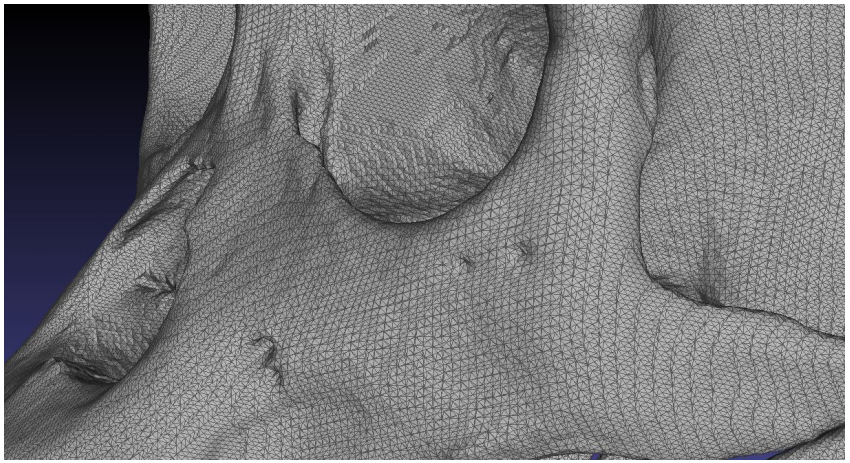

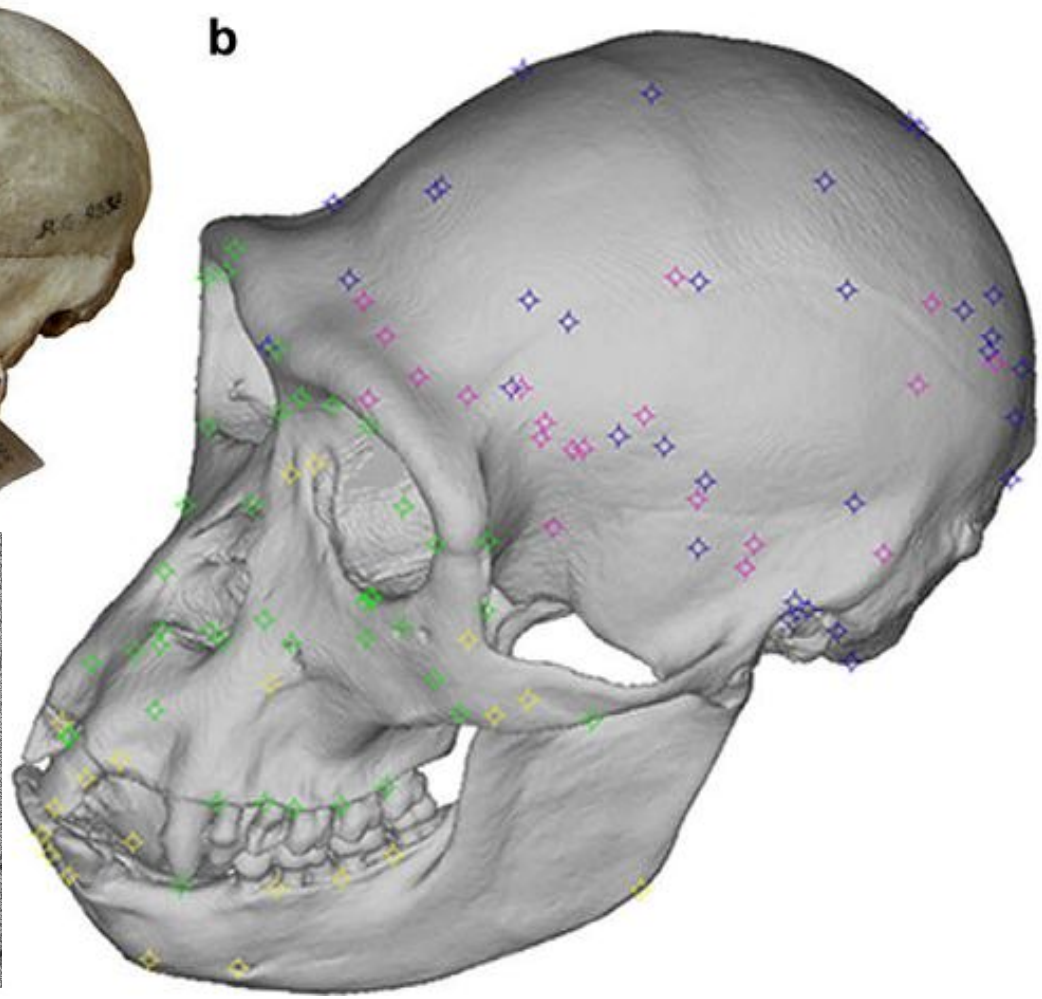

Pan paniscus

- Manual localization of the initial deformable surface (a small sphere) in the middle of the endocranial cavity
- **No user interaction**
- **Manage automatically the "holes"** (foramen, optic nerves…)

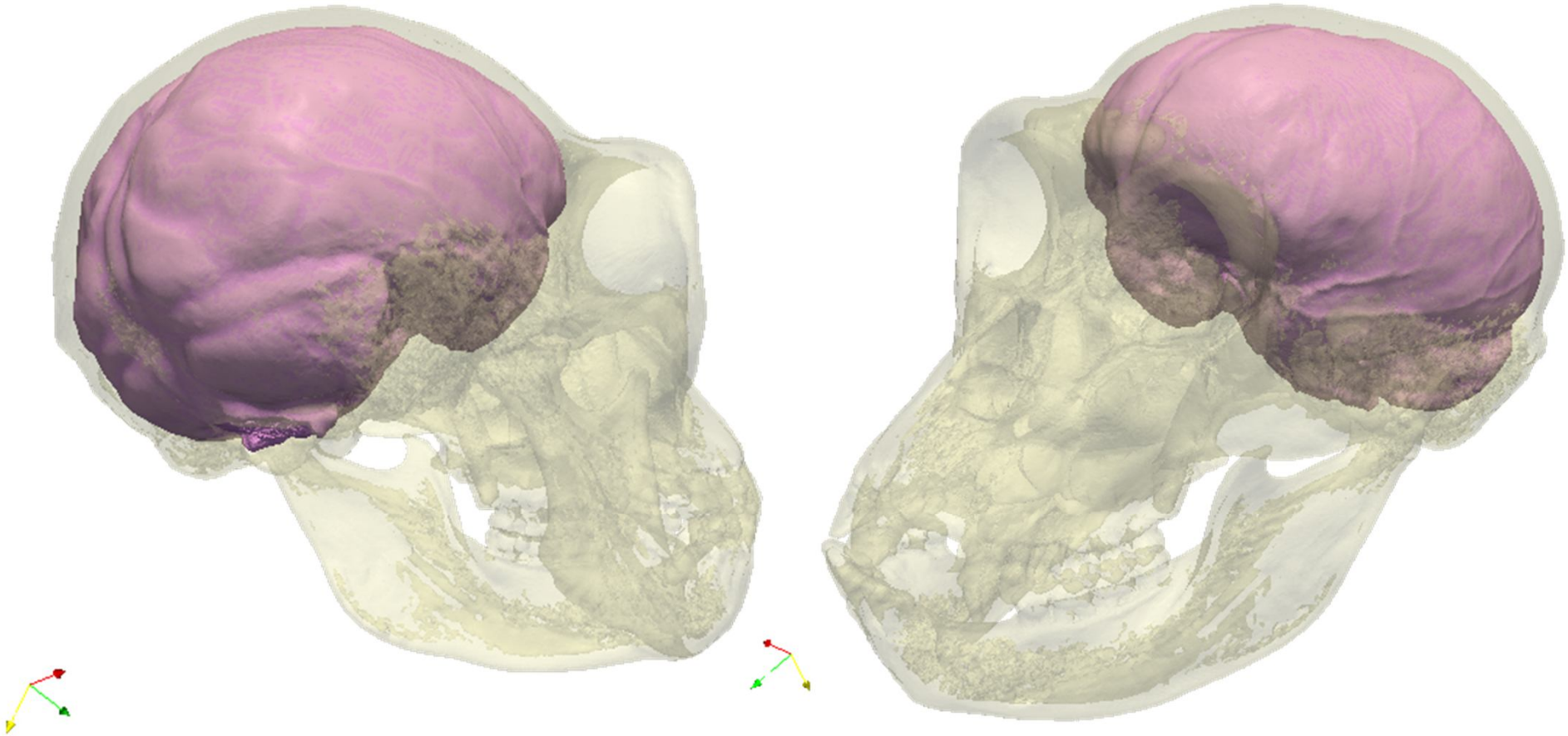

Pan paniscus

A. Balzeau, E. Gilissen et al. "Internal cranial anatomy of the type specimen of Pan paniscusand available data for study". Journal of Human Evolution 56, 205–208 (2009) (418 cm^3)

Our segmentation (410 cm^3)

Pan troglodytes

- CT-Scan of a skull: 209 slices of 512 × 512 pixels
- Resolution: 0.461 × 0.461 × 0.600mm

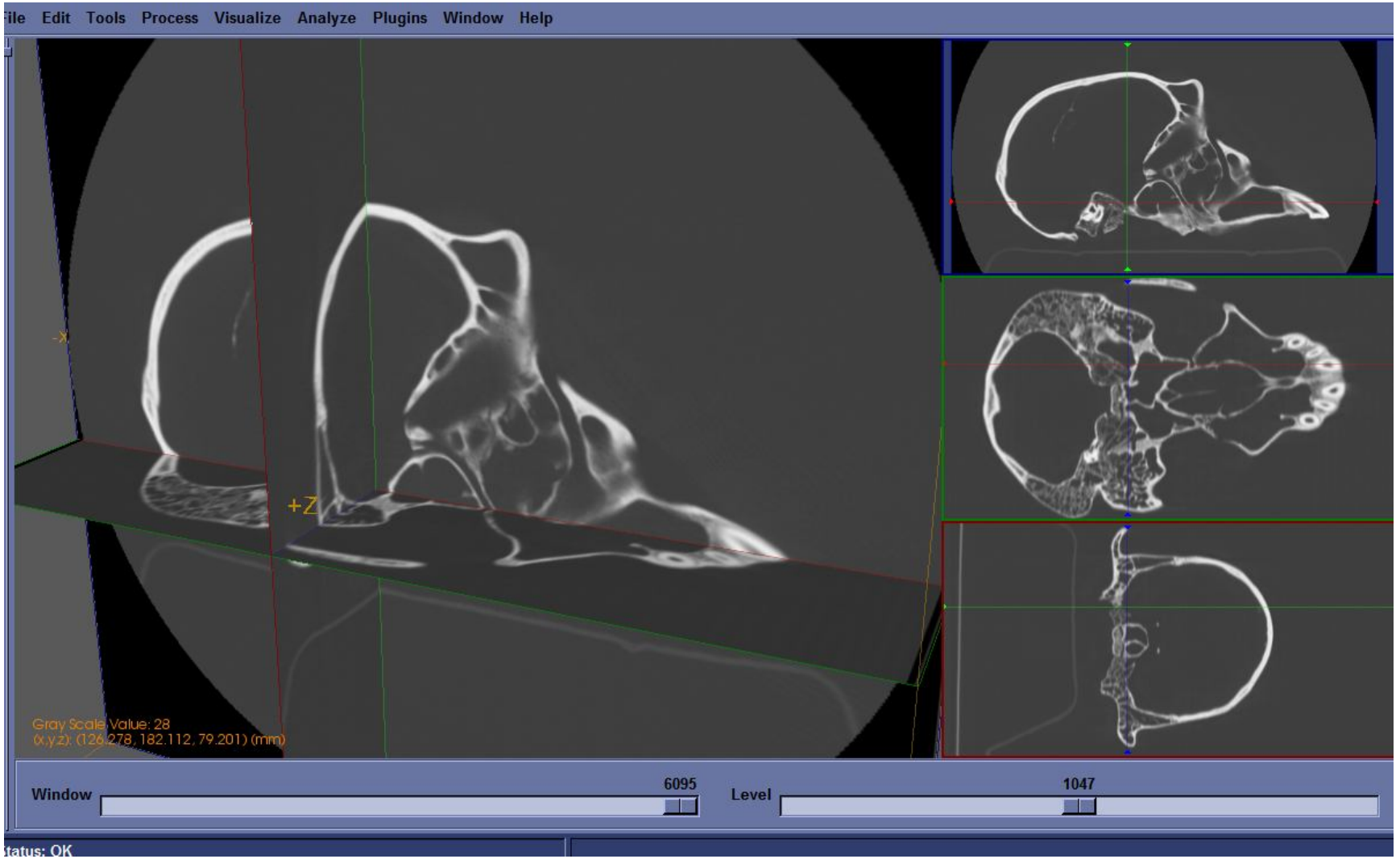

Pan troglodytes

- Automatic extraction of the bony surface by thresholding
- Data: 749,560 points

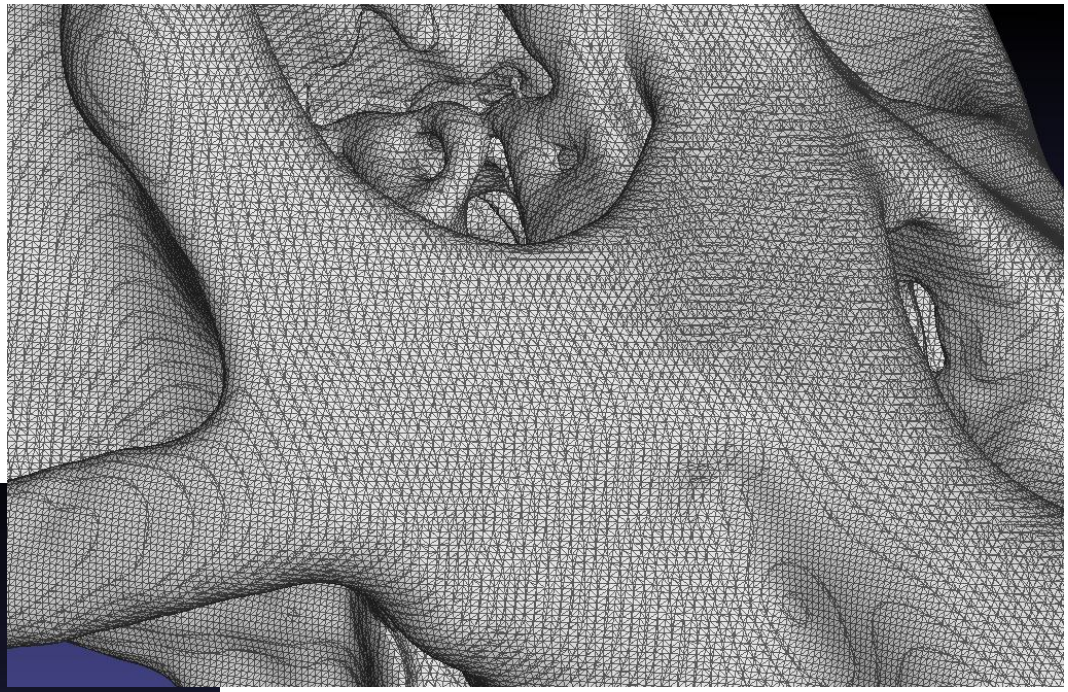

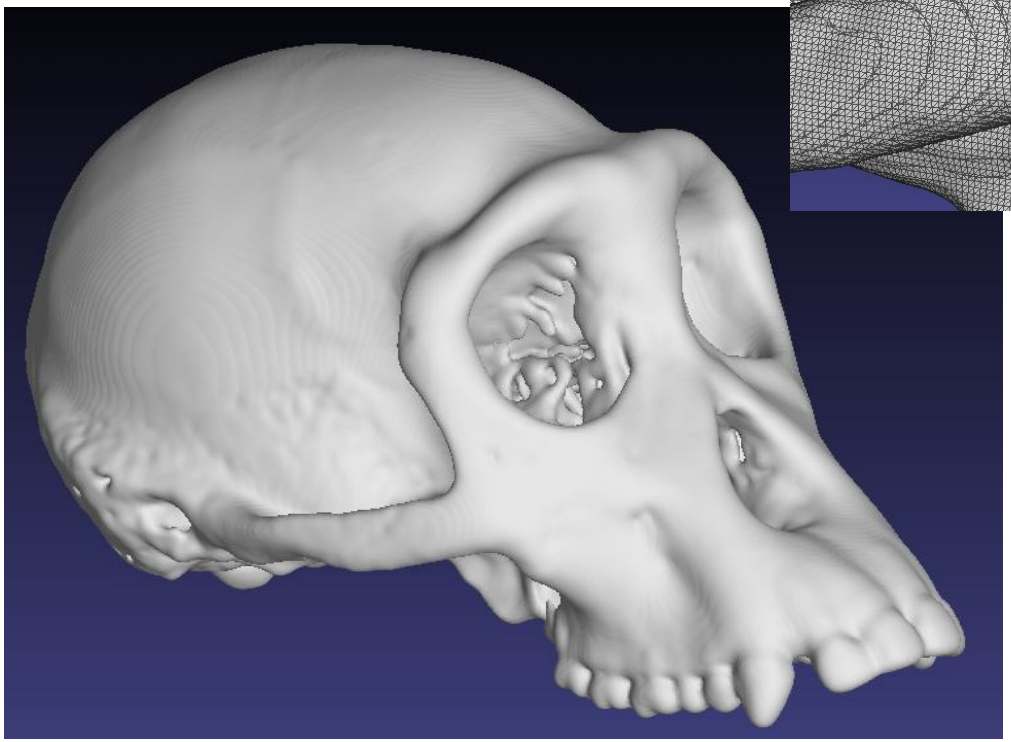

Pan troglodytes

- Manual localization of the initial deformable surface
- No user interaction
- 398,942 vertices / 797,880 faces

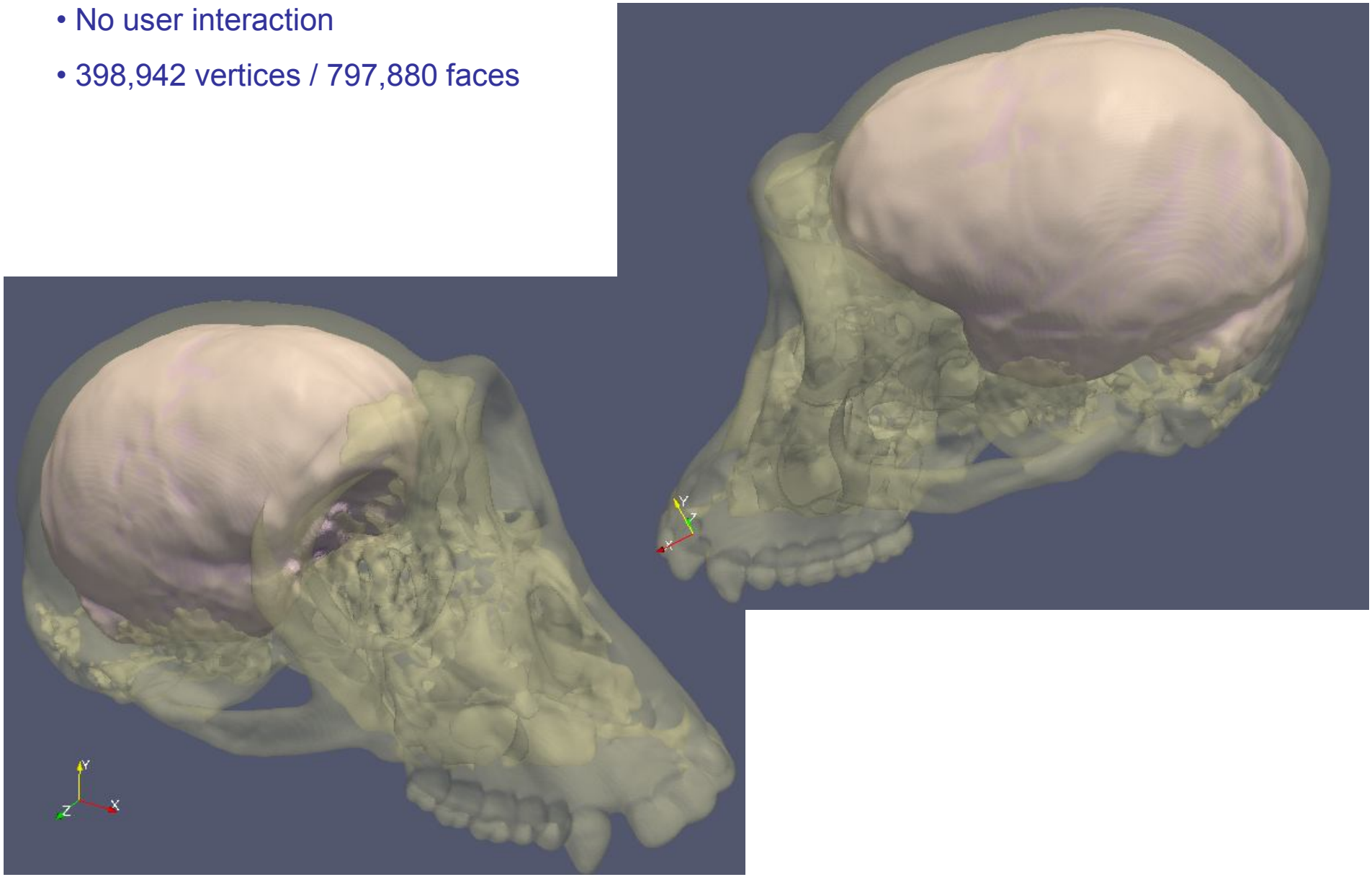

Australopithecus africanus STS5

- CT-Scan of the fossil: 998 slices of 512 × 512 pixels
- Resolution: 0.348 × 0.348 × 0.200 mm

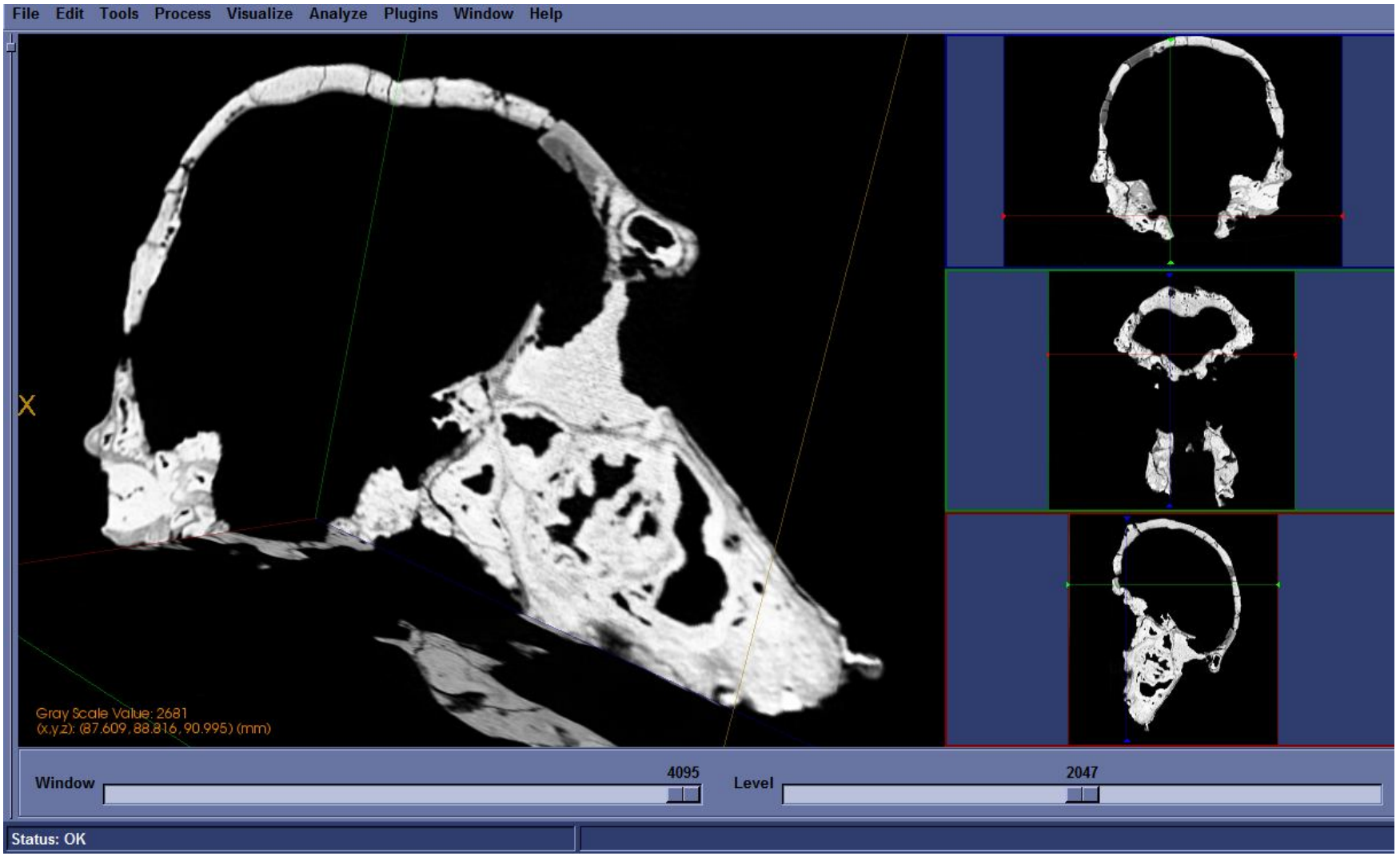

Australopithecus africanus STS5

- Automatic extraction of the bony surface by thresholding
- Data: 635,096 points

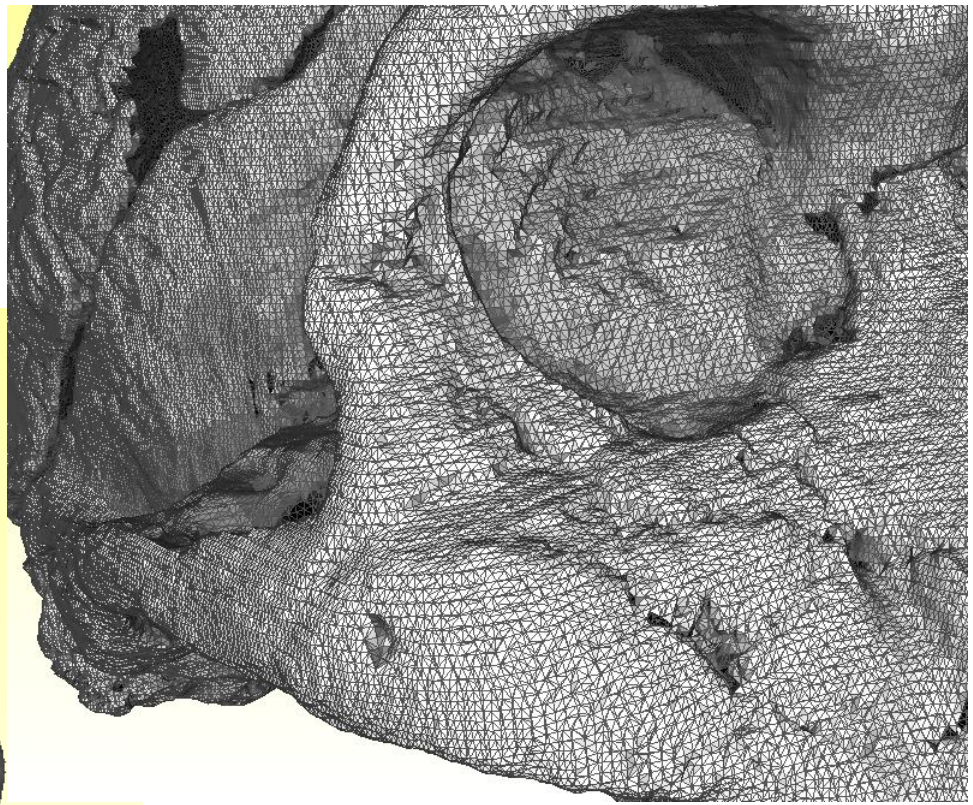

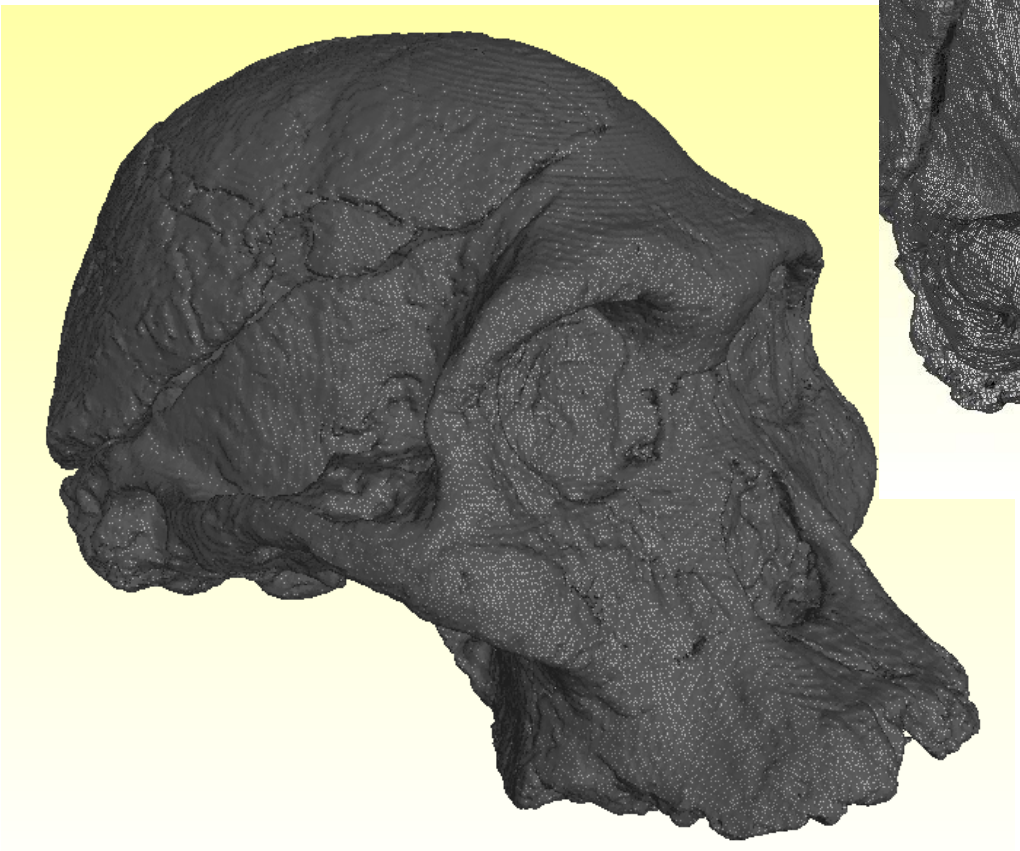

Australopithecus africanus STS5

- Manual localization of the initial deformable surface
- No user interaction
- 401,960 vertices / 803,916 faces

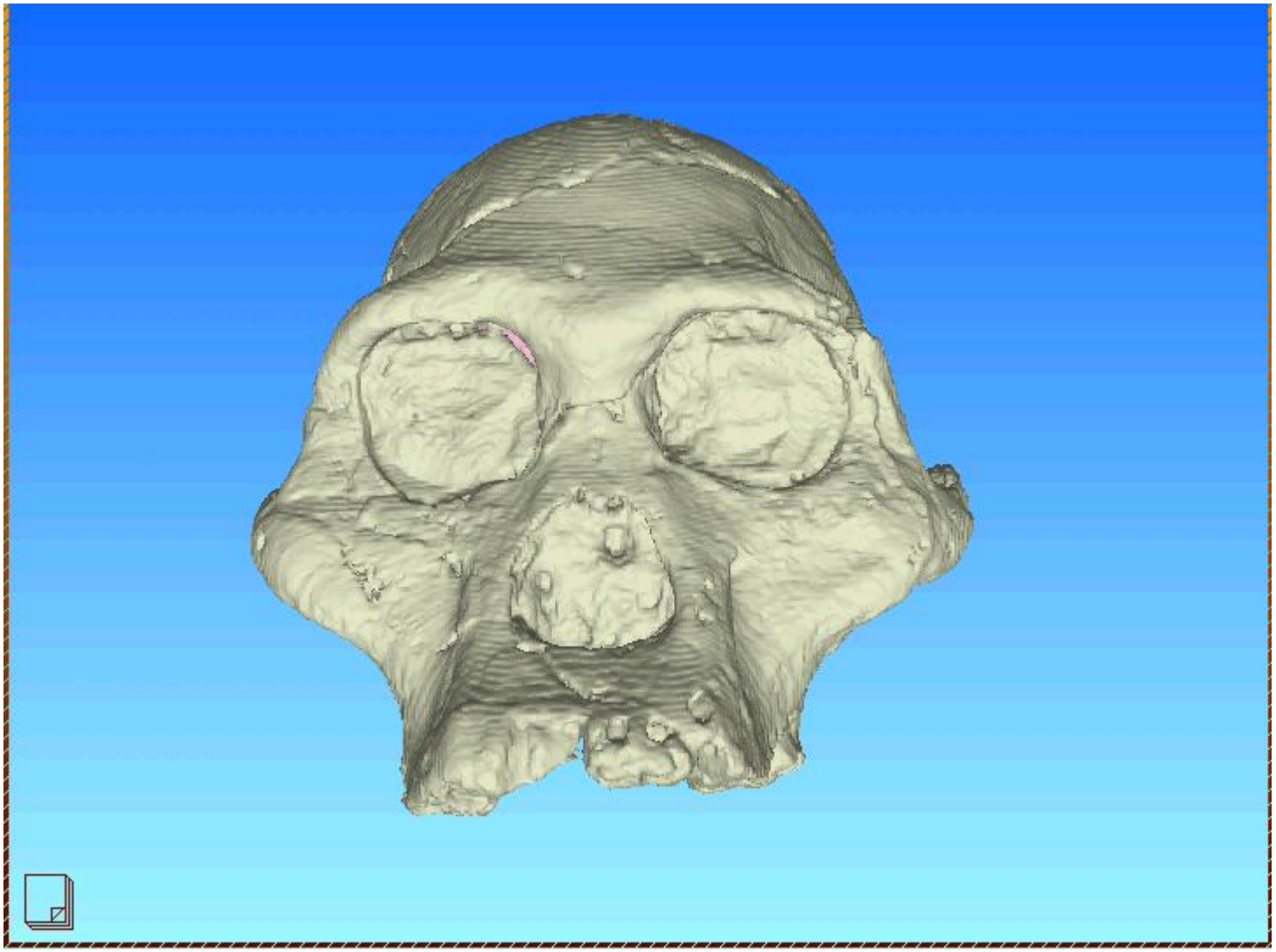

Australopithecus africanus STS5

R. Holloway et al. "The Human Fossil Record". Vol. III. Wiley (2004) (485 cm^3)

Our segmentation (476 cm^3)

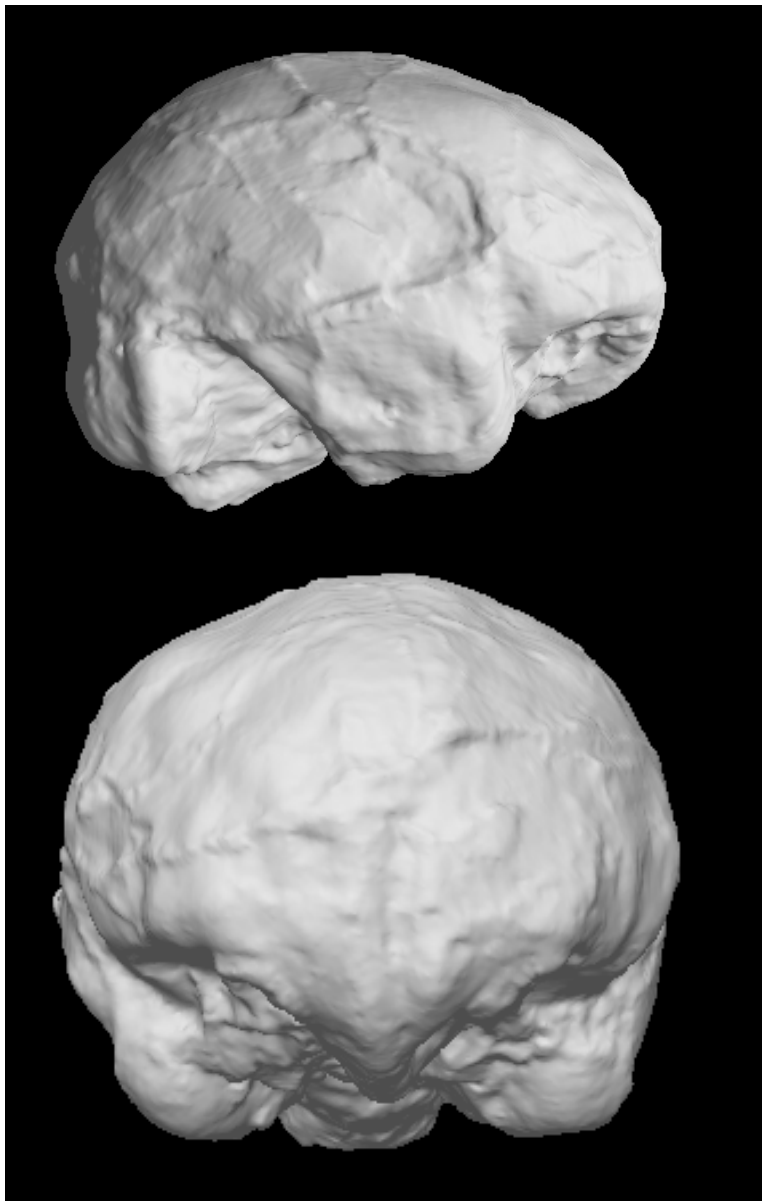

Australopithecus africanus STS5

D. Falk et al. "The Brain of LB1, Homo floresiensis". Science, 308, 242 (2005) – Supporting Online Material (473 cm^3).

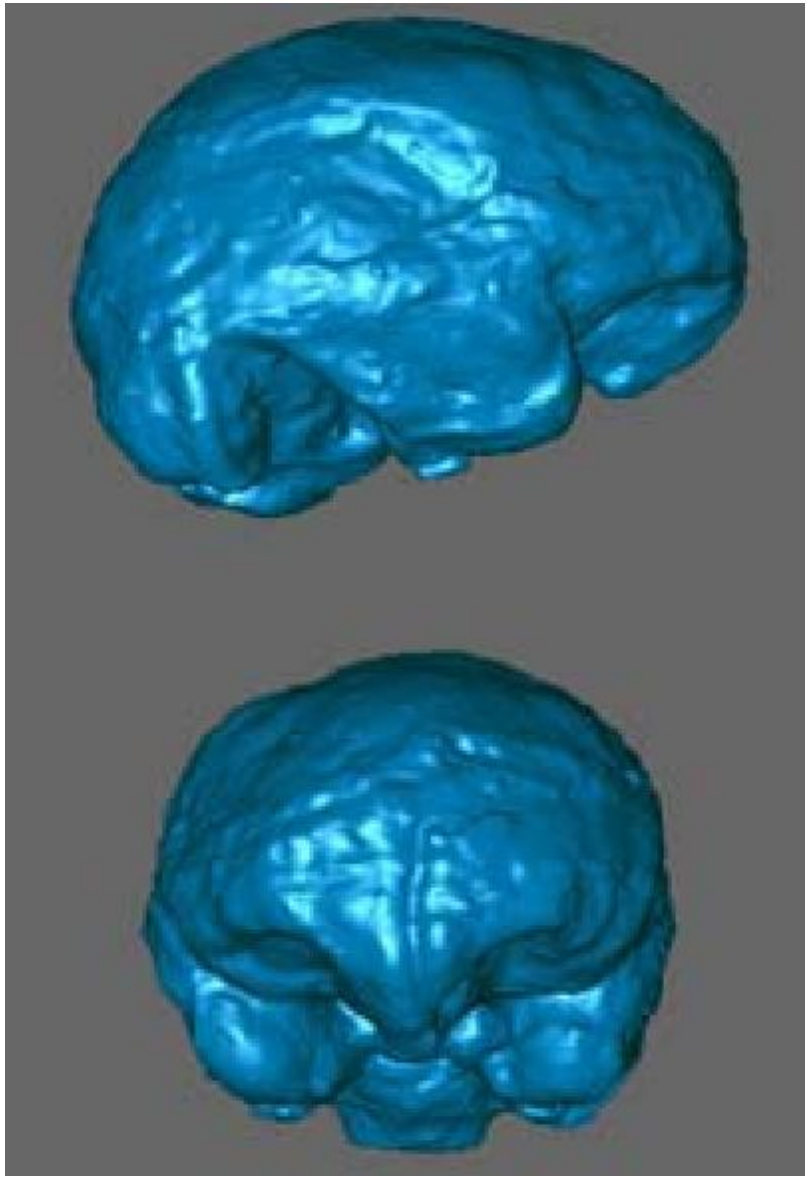

Our segmentation (476 cm^3)

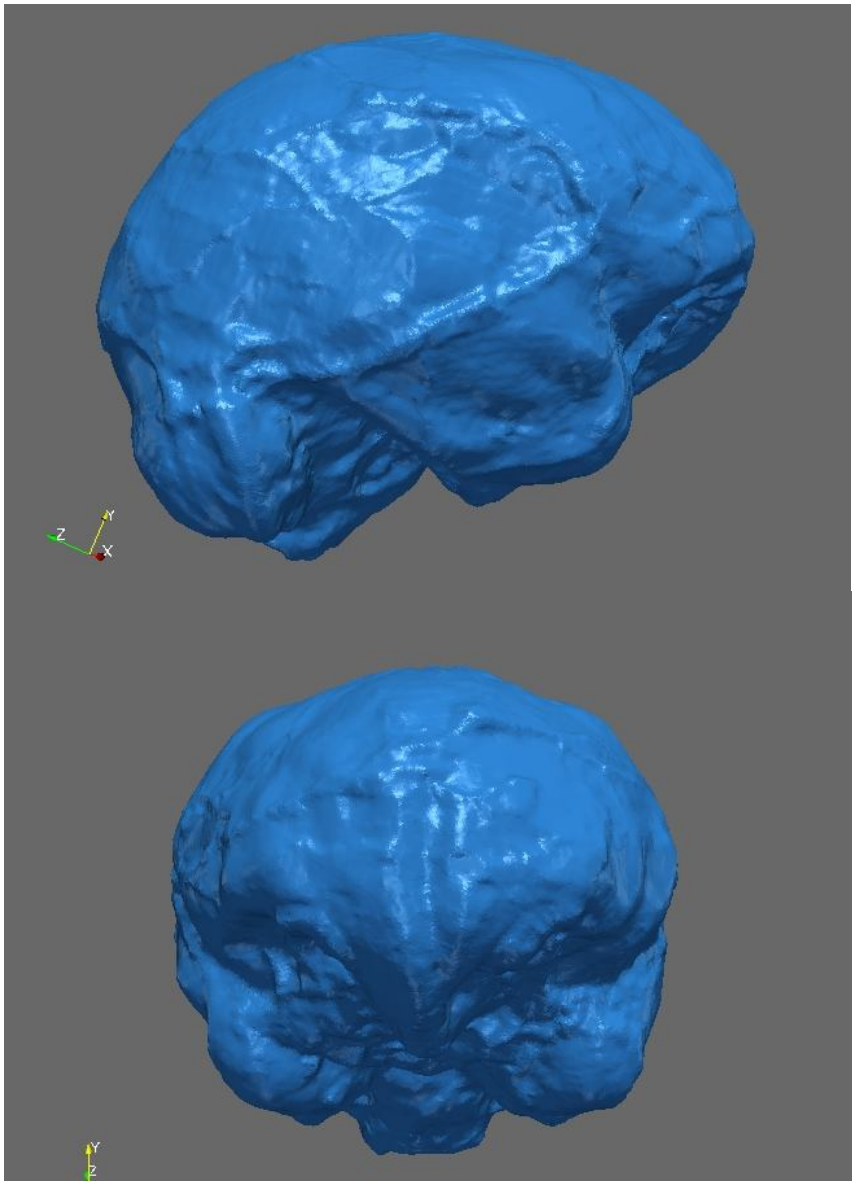

A computer-assisted segmentation by J. Braga (468 cm³)

Our segmentation (476 cm³)

STS5

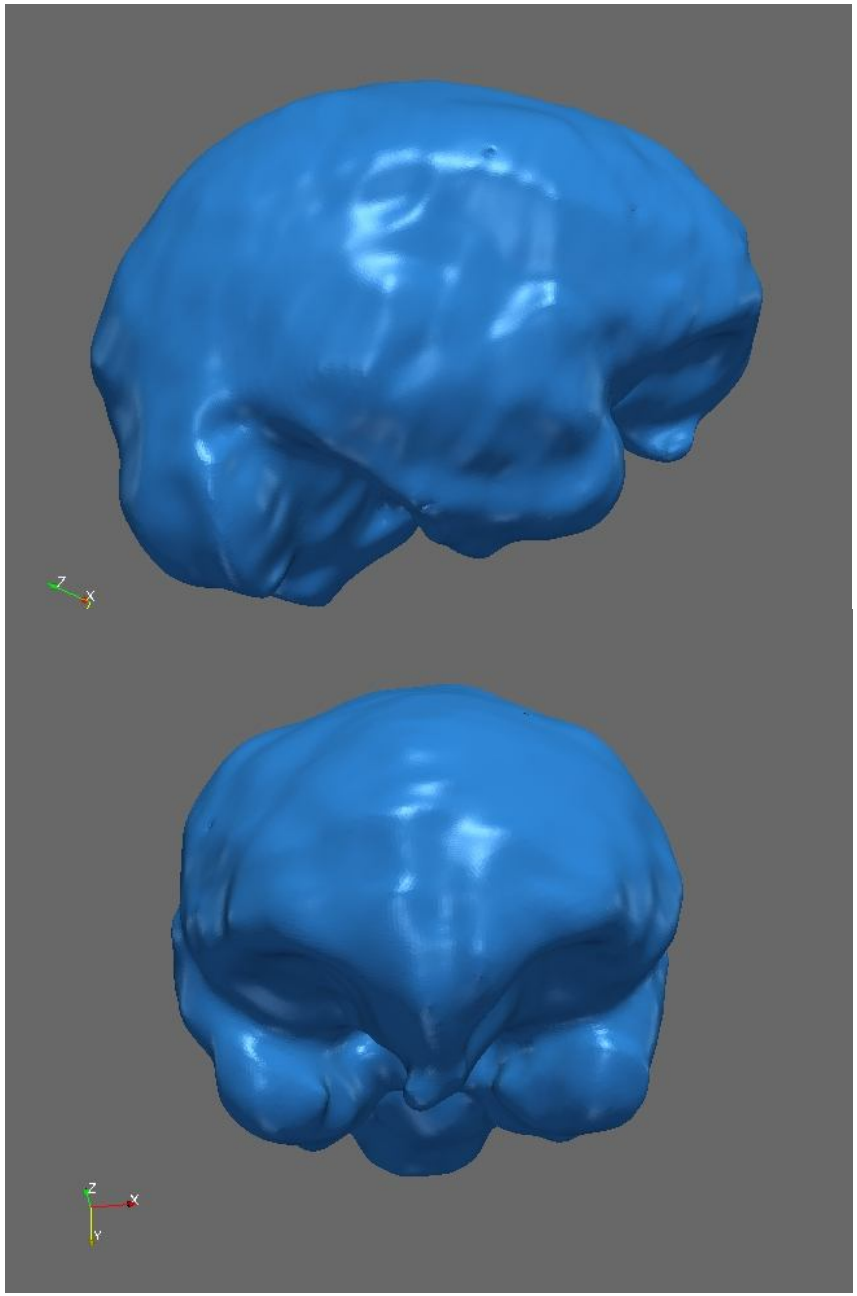

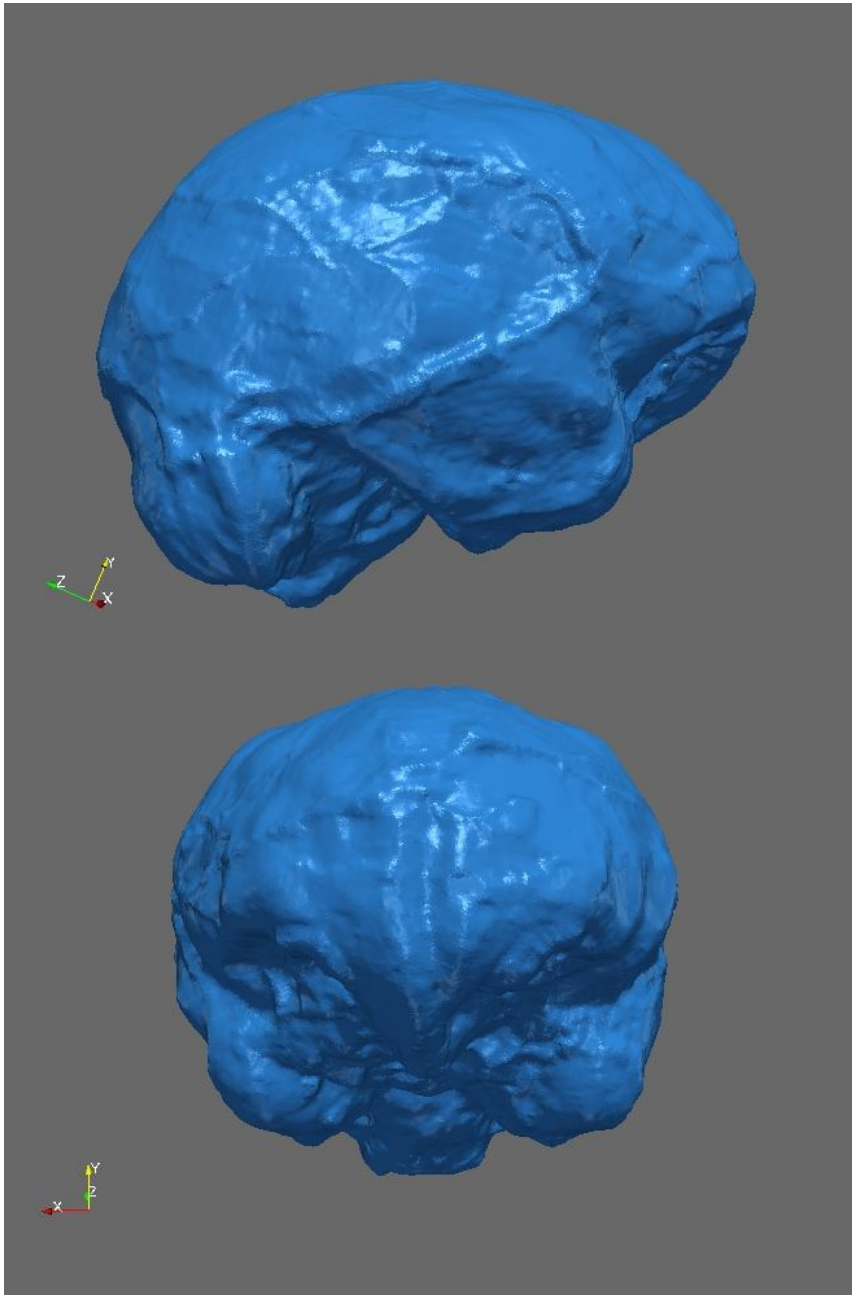

In-vivo data

- CT-Scan of the head of a child affected by a plagiocephaly (asymmetrical distortion of the skull): 153 slices of 512 × 512 pixels
- Resolution: 0.488 × 0.488 × 1.250 mm

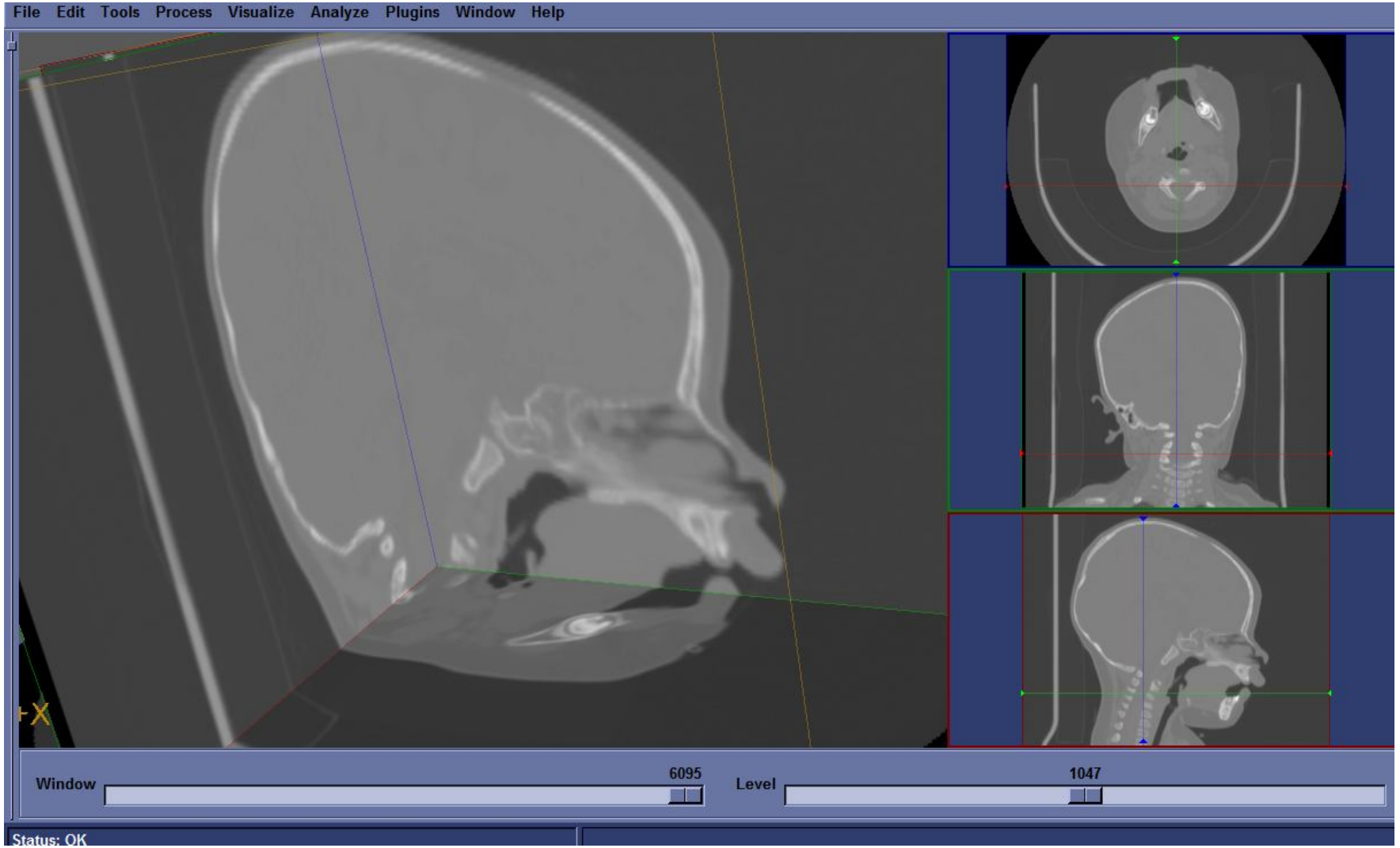

In-vivo data

- Manual localization of the initial deformable surface
- No user interaction
- **Manage automatically the fontanels**
- 364,721 vertices / 729,438 faces
- Could be useful to **compare the dissymmetry of the endocranium and of the skull base**

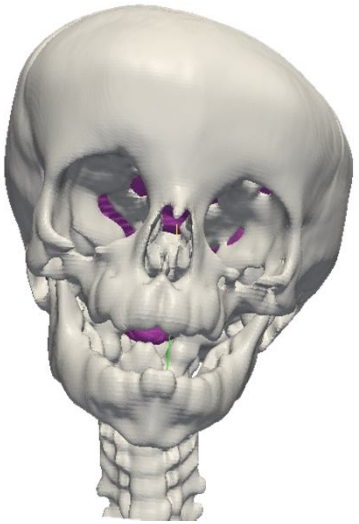

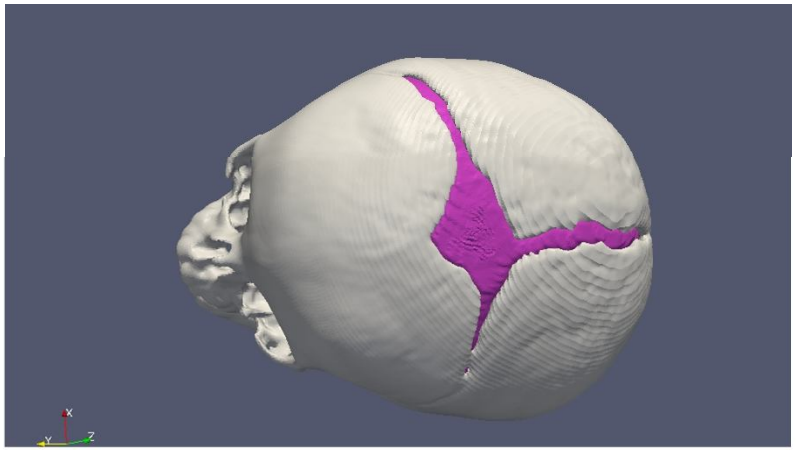

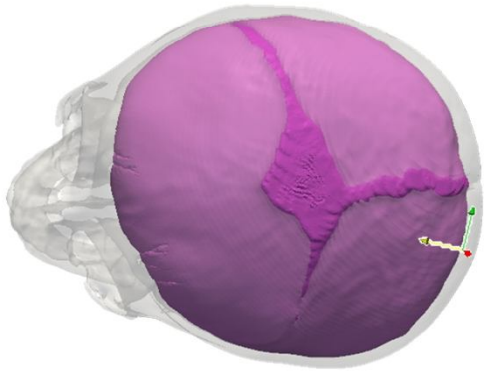

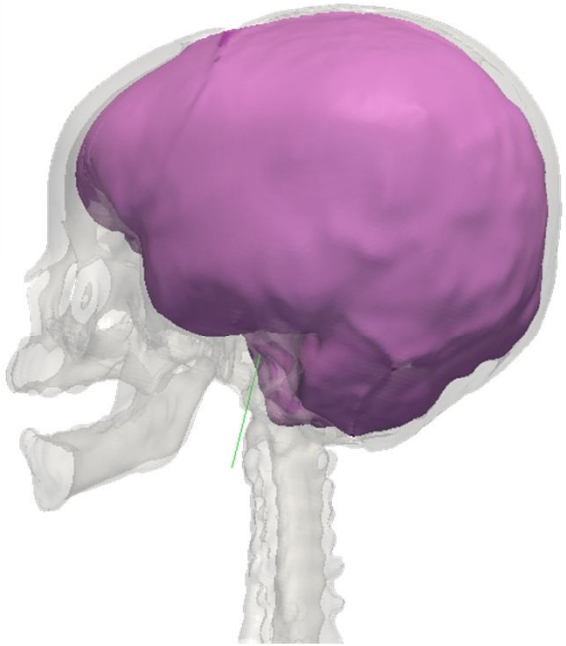

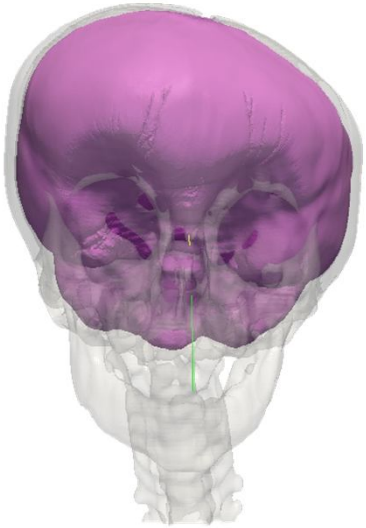

Conclusion

Today

- Encouraging preliminary results on dry samples, fossils and in-vivo data
- To be assessed w.r.t. to real (photographs, real casts) and virtual (virtual endocasts) data by computing quantitative parameters (not only volumes but also lengths, landmark positions, etc.)
- To be tested on large databases (e.g. primates, in-vivo CT) and other fossils: STS71, SK48…

Short term

- To accelerate the process by at least $\times 10$ to $\times 100$
- To improve the automatic refinement of the mesh around the complex shaped parts
- To develop the graphical interface in order to be used by non-specialists

$\Rightarrow$ **make a first version of the software available to the research community (paleo-anthropology, in medicine, in computer science) next year.**

Mid-term

- To label parts of the deformable surface
  $\rightarrow$ automatic decomposition into lobes or functional areas
- To insert the surface directly into the CT image and use density profiles instead of points
  $\rightarrow$ matrix/bone differentiating

Acknowledgments

This work is partially supported by the INRIA Collaborative Research Initiative 3D-MORPHINE.

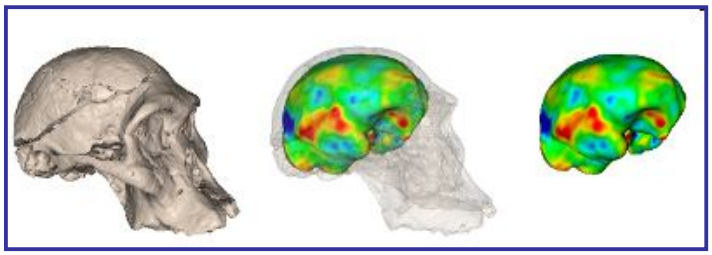

INRIA

Many thanks to the students of IUT Arles who participated to the development of the software:

2009-2010

- *Clément WELSH*
- *Irwin SCHLAEFLIN*
- *Vincent LECOINTRE*
- *Gaël VALNET*
- *Yoan VERGEOT*

2008-2009

- *Pierre SCIONICO-GUESNOT*
- *Romain CHARBIT*
- *Thibault VENET*